THESIS FOR THE DEGREE OF LICENTIATE OF ENGINEERING

# Cellulose in quaternary ammonium hydroxide solutions
# Properties and Functionalisation

SHIRIN NASERIFAR

Department of Chemistry and Chemical Engineering

CHALMERS UNIVERSITY OF TECHNOLOGY

Gothenburg, Sweden 2022

Cellulose in quaternary ammonium hydroxide solutions

Properties and Functionalisation

SHIRIN NASERIFAR



Licentiatuppsatser vid Institutionen för kemi och kemiteknik
Chalmers tekniska högskola.
Nr 2022:02

Department of Chemistry and Chemical Engineering

Chalmers University of Technology

SE-412 96 Gothenburg

Sweden

Telephone +46 (0)31-772 1000

Cover: *In-situ* IR monitoring of cellulose etherification, microscopy image of pulp ballooning in *N,N*-dimethylmorpholinium hydroxide(aq)

Printed by Chalmers Reproservice

Gothenburg, Sweden 2022

# Cellulose in quaternary ammonium hydroxide solutions

Properties and Functionalisation

SHIRIN NASERIFAR

Department of Chemistry and Chemical Engineering

Chalmers University of Technology

## Abstract

An ever-increasing demand to shift away from fossil-based feedstock towards renewable resources has led to more use of bio-based materials. Cellulose being the most abundant biopolymer on Earth has received a considerable attention with a wide range of applications (in textile fibers, films, membranes, etc.), many of which requiring processing through dissolution and/or chemical functionalisation. Cellulose cannot melt when heated or dissolve in the most common aqueous and organic solvents. Thus, a lot of efforts have been made to develop new and effective solvents aiming to address some common limitations associated with the existing solvents including solution instability, low dissolution capacity, specific temperature requirement, side reactions of the solvent itself and narrow concentration range required for the dissolution.

Water solution of quaternary ammonium hydroxides (QAHs), classified as relatively green and economical chemicals, show promising potential in cellulose dissolution. In this thesis, to gain deeper insight on QAHs(aq) as derivatisation and dissolution media for cellulose, cellulose etherification in benzyltrimethylammonium hydroxide (Triton B) and tetramethylammonium hydroxide (TMAH), along with NaOH(aq) as well as different mixtures of these bases was investigated. In this study the emphasis was set on *in-situ* monitoring of the etherification reaction combined with the spectroscopic analysis of the products. The results highlighted the impact of hydroxide base composition on cellulose etherification where QAHs either alone or in combination enhanced the reagent solubility and cellulose solution stability during the reaction compared to NaOH which resulted in a lower solution stability promoting likely side reactions of the introduced substituents. Considering the importance of the dissolution system on functionalisation, a new solvent for cellulose was developed in the next study inspired by the well-known industrially used solvent *N*-methylmorpholine *N*-oxide (NMMO). In this study, *N,N*–dimethyl morpholinium and hydroxide ions were coupled to synthesize *N,N*-dimethylomorpholinium hydroxide(aq), and the dissolution properties of cellulose in the new solvent were investigated showing mostly molecularly dissolved cellulose chains with good chemical stability upon refrigeration.

**Keywords**: cellulose, quaternary ammonium hydroxides, dissolution, etherification, Triton B, TMAH, NaOH, *N,N*-dimethylmorpholinium hydroxide

# List of Publications and presentations

This thesis is based on the following papers:

Paper I. ***In-situ* monitoring of cellulose etherification in solution: probing the impact of solvent composition on the synthesis of 3-allyloxy-2-hydroxypropyl-cellulose in aqueous hydroxide systems**
Shirin Naserifar, Paul Kuijpers, Sylwia Wojno, Roland Kádár, Diana Bernin, Merima Hasani
Manuscript

Paper II. ***N,N*-dimethylmorpholinium hydroxide as a novel solvent for cellulose**
Shirin Naserifar, Beatrice Swensson, Diana Bernin, Merima Hasani
European Polymer Journal, 161, 2021, 110822.

# Part of the work has been presented by **Shirin Naserifar** at:

- WWSC Workshop June 2020 (poster presentation)
- WWSC Workshop November 2020 (poster presentation)
- WWSC Workshop June 2021 (poster presentation)
- The 7th EPNOE International Polysaccharides Conference Nantes, France, 11-15 October 2021 (oral presentation)
- WWSC Workshop November 2021 (poster presentation)

## Contribution Report

The author's contribution to the papers included in this thesis:

Paper I. The author designed and carried out all the experimental work except for the rheology measurements, which were carried out at the materials engineering department by Sylwia Wojno and Roland Kádár and interpreted and written by them. In addition, NMR measurements were run at Swedish NMR centre and partly interpreted by co-supervisor Diana Bernin. Paul Kuijpers, a consultant in Metler-Toledo, contributed to the design of some *in-situ* IR study experiments and interpretation of the results. The author was responsible for evaluation of results and writing of the manuscript with support from Merima Hasani (main supervisor) and Diana Bernin (co-supervisor).

Paper II. The author designed and carried out all the experimental work except for some of NMR measurements which were run by co-supervisor Diana Bernin at Swedish NMR centre and DLS which were run and interpreted by Beatrice Swensson. The author was responsible for evaluation of results and writing the manuscript except for DLS (written by Beatrice Swensson) with support from Merima Hasani (main supervisor) and Diana Bernin (co-supervisor).

## List of abbreviations

| | |
|---|---|
| AGU | anhydroglucose unit |
| AGE | allyl glycidyl ether |
| AHP-cellulose | 3-allyloxy-2-hydroxypropyl-cellulose |
| ATR-FTIR | attenuated total reflectance Fourier transform infrared |
| CA | cellulose acetate |
| CMC | carboxymethyl cellulose |
| $CS_2$ | carbon disulfide |
| DMAc/LiCl | *N,N*-dimethylacetamide/lithium chloride |
| DMAP | 4-dimethylaminopyridine |
| DMSO | dimethyl sulfoxide |
| DLS | dynamic light scattering |
| DP | degree of polymerization |
| GTAC | glycidyltrimethylammonium chloride |
| HPC | hydroxypropyl cellulose |
| HSQC | heteronuclear single quantum coherence |
| IL | ionic liquid |
| MC | Methyl cellulose |
| MCC | microcrystalline cellulose |
| MS | molar substitution |
| MW | molecular weight |
| NDMM-OH | *N,N*-dimethylmorpholinium hydroxide |
| NMMO | *N*-methylmorpholine N-oxide |
| NMR | nuclear magnetic resonance |
| PD | polydispersity |
| PEG | polyethylene glycol |
| QAH | quaternary ammonium hydroxide |
| SEC | size exclusion chromatography |
| TBAH | tetrabutylammonium hydroxide |
| TEAOH | tetraethylammonium hydroxide |

| | |
|---|---|
| TMAH | tetramethylammonium hydroxide |
| Triton B | trimethylbenzylammonium hydroxide |

# Contents

# 1 Introduction

In today's world, dramatic increase in population and the ongoing use of petroleum-based resources to satisfy human needs have resulted in environmental challenges. The majority of industries rely on fossil-based resources to produce their everyday-use products. In recent decades, there has been a growing necessity to shift from fossil resources to renewable alternatives that are sourced from biomass in order to meet the humankind's increasing material and chemical needs. In this regard, cellulose as the most abundant biopolymer on Erath, has received increasing attention. The market for cellulose has maintained a steady growth over the past decades due to its various applications in different end-use products including paper and paper boards, textiles, cellulose derivatives (in food, pharmaceutics, etc.), nano- and microcellulose, etc. Therefore, an ever-increasing need for cellulose application in several areas promotes the aiming at a broad toolbox for its structural modification research.

However, cellulose can neither melt when heated nor dissolve in the most conventional organic and aqueous solvents, which makes its processing challenging for many applications. A number of solvents have been reported to be capable of dissolving cellulose, some of which are already in use on an industrial scale for instance aqueous carbon disulfide-sodium hydroxide ($CS_2$-NaOH(aq)) and *N*-methylmorpholine *N*-oxide (NMMO). However, the existing disadvantages such as toxicity, instability, low dissolution capacity, undesired reactions and cellulose degradation have called for more research to be carried out with the aim of overcoming these drawbacks and developing novel solvents with improved capabilities.

In addition, cellulose has three reactive OH groups, which open up the opportunity to modify it and create a vast number of derivatives with various properties and applications. Among cellulose derivatives, cellulose ethers have gained a lot of attention due to their non-toxicity and very often solubility in water. A lot of research has been carried out on cellulose ethers, however, there remains a lack of comprehensive understanding of the course of the etherification. This is especially in regard to numerous side reactions readily taking place in the aqueous processing media and the potential to adjust these to control the products' properties. One major difficulty

contributing to poor understanding regarding the course of etherification is a challenging *in-situ* monitoring of these reactions. Therefore, in the presented work efforts have been made to developing and investigating a methodology for *in-situ* monitoring of cellulose etherification in a dissolved state. In parallel, having the importance of cellulose solvent highlighted, a study was conducted on developing a new solvent for cellulose, whether for functionalisation or regeneration applications.

## 1.1 Objectives

The overarching goal of this thesis was to investigate and gain deeper insight into quaternary ammonium hydroxides as solvents, as well as etherification media for cellulose. Specifically, the conducted studies have aimed at:

- Development of a methodology for *in-situ* monitoring of cellulose etherification in the dissolved state
- Gaining insight into the influence of the solvent composition on the course and outcome of etherification
- Development of a novel solvent applicable to regeneration or functionalisation of cellulose.

In the first study, two well-known aqueous quaternary ammonium hydroxides namely Tetramethylammonium hydroxide (TMAH) and benzyltrimethylammonium hydroxide (Triton B) were investigated as etherification media for cellulose, both individually and in combination with each other or NaOH(aq). Since the critical role of the solvent was highlighted in the first study, in continuation, in the second study the emphasis was put on developing a new aqueous quaternary ammonium hydroxide solvent—*N,N*-dimethylmorpholinium hydroxide (NDMM-OH(aq))—to enhance cellulose dissolution and detailed dissolution analysis were carried out.

# 2 Cellulose

The first discovery of cellulose dates back to 1838 by a French chemist Anselme Payen who noticed a solid fibrous material remaining after acid or ammonia treatment of plant tissue and subsequent water, alcohol and ether extraction[1,2]. Later he used elemental analysis and determined its chemical formula to be $C_5H_{10}O_5$. The term "cellulose" was used for the first time in a report on Payen's work in 1839[3]. Polymer structure of cellulose was discovered by Hermann Staudinger in 1920[4] and today it is well-known as a linear homopolysaccharide. Cellulose is the most abundant biopolymer on Earth, existing not only in plants as the main component of the plant cell wall but also in some living organisms such as algae, tunicate, and bacteria.

## 2.1 Cellulose morphology and structure

Independent of its biological sources, cellulose consistently has the same molecular structure. It is composed of D-anhydroglucose units (AGU) connected via β-1,4-glycosidic linkages with every second AGU being rotated 180 °C around these linkages (figure 1). The number of connected D-glucose units is defined as the degree of polymerization (DP), which can vary from 1,000 to 20,000, depending on its biological sources[5]. The two ends of a cellulose chain are chemically different as one of them is non-reducing (with its anomeric carbon atom involved in a glycosidic bond) and the other is reducing, comprising of a free anomeric carbon prone to conversion to an aldehyde.

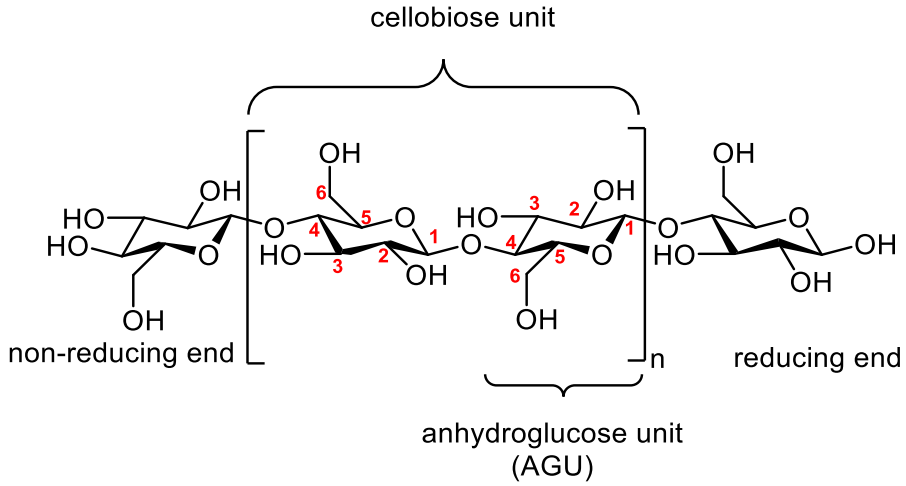


*Figure 1. Cellulose chain structure*

Each AGU in the cellulose chain carries three equatorial OH groups located on C2, C3 and C6 positions, some of which contribute to intra- and inter-molecular H-bonds, both along and between the chains. Intramolecular H-bonds are formed between C3 hydroxyl groups and the ring oxygen in the adjacent AGU, as well as C2 hydroxyl groups and the hydroxyl group on C6 position at the adjacent AGU[6]. Interchain hydrogen bonds are formed between hydroxyl group on C6 and hydroxyl group on C3 of the neighboring chain (figure 2). Flat chain conformation of cellulose is stabilized via intramolecular hydrogen bonds, which contributes to chain stiffness and results in a high tendency to crystallization. While intermolecular hydrogen bonds cause a sheet-like structure by alignment of cellulose chains next to each other. In addition, hydrogens are axially linked to the carbons of the pyranose ring, which create more hydrophobic regions below and above the ring planes, promoting hydrophobic interactions between sheets when stacking on top of each other into semi-crystalline structures called microfibrils. Therefore, cellulose is a polymer with an amphiphilic structure. In native cellulose, organization of cellulose chains into microfibrils is determined by biosynthesis and it is important to note that cellulose structure is not fully crystalline, in fact it contains less-ordered regions, which is why microfibrils are considered semi-crystalline. A model explaining how these crystalline and amorphous regions exist together is called fringed fibrillar model[7], which is widely accepted for cellulose suprastructure in nature (figure 3). These semi-crystalline microfibrils are further packed into larger aggregates in the cell wall called macrofibrils.

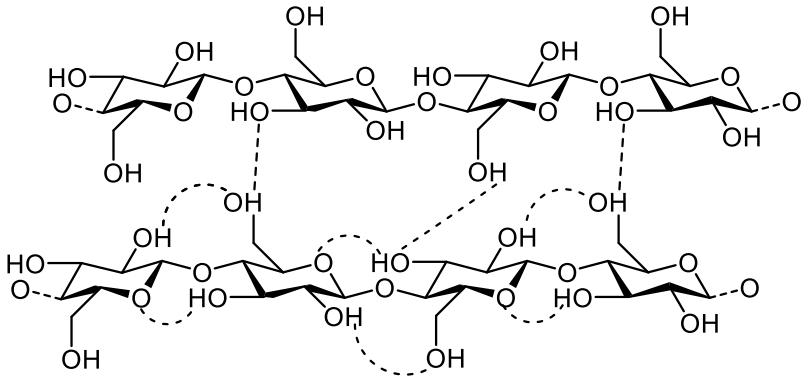

*Figure 2. Inter-and intramolecular H-bonds in cellulose structure*

Crystalline structure of cellulose has been studied extensively, leading to the discovery of four main crystalline allomorphs namely Cell I, II, III and IV. Cell I is the native structure of cellulose that is formed during biosynthesis. Solid state NMR spectroscopy has shown that Cell I exists in two different allomorphs: Iα and Iβ. Iα can be found in bacteria and algae, and Iβ is the dominant structure in higher plant cell wall. X-ray and neutron diffraction studies suggest that Iα occupies a triclinic space while Iβ has a monoclinic structure[8]. Cell II as the thermodynamically more stable crystalline structure is formed when native cellulose (Cell I) is treated with alkali or regenerated from a dissolved state [9]. In Cell I the polymer chains have parallel configuration, while in Cell II they transform to an antiparallel arrangement. Cell III is obtained by treatment of native cellulose with liquid ammonia or anhydrous ethylamine, while Cell IV can be obtained via different chemical treatments at a high temprature[10,11].

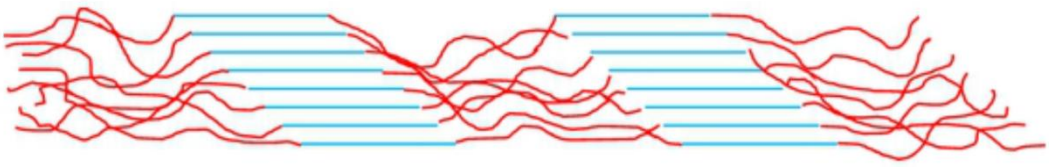

*Figure 3. Cellulose chains organization in a microfibril illustrated by Khazraji et al.*[12]

Cellulose exists rather purely in cotton occupying approximately 90% of the total composition, however, it is mostly found along with other components such as lignin, hemicellulose and small amounts of low molecular compounds called extractives[13]. Lignin provides a mechanical strength, barrier against microbial attacks and enables liquid transportation through hydrophobization[14,15]. The role of hemicellulose is not fully understood; however, it is believed to have regulatory functions. To isolate cellulose, different pulping processes are used, in which cellulose fibres with different strengths and purity are delignified. Mechanical pulp such as sulfite pulp typically contains around 20-25% residual lignin[16] and is used in products that need sheet formation and moderate strength such as newsprint furnish. Dissolving pulp qualities have a higher cellulose content with the lignin, hemicellulose and extractive content less than 10% in total[17]. These dissolving pulps are used to produce regenerated cellulose

(e.g., textile fibres and films) and cellulose derivatives. As mentioned previously, DP of cellulose depends on its original source and is reduced to 300-1700 AGUs upon pulping[18].

## 2.2 Cellulose reactivity and accessibility

The reactivity of cellulose primarily depends on the inherent chemical reactivity of its alcohol groups (three hydroxyl groups on each AGU, one primary hydroxyl on C6 and two secondary ones on C2 and C3) and their accessibility, which play a significant role in chemical modification and dissolution. Furthermore, cellulose accessibility is affected by a number of parameters such as the size of the pores in the cellulose structure, internal accessible surface (determined by size of the fibrils) and aggregated fibrils, size and type of the reagent and solvent and cellulose supramolecular structure[19]. Therefore, the main challenge for efficient chemical modification of cellulose is to achieve appropriate accessibility of the hydroxyl groups either by complete dissolution (which is not possible in the regular solvents) or suitable pretreatments prior to performing a heterogeneous modification in a solid state or suspension. In order to promote the accessibility of cellulose, the pores must be kept open, the fibrillar aggregates must be interrupted and the crystalline regions must be altered[20].

In recent decades, some methods have been used as pretreatment of cellulose prior to its further processing, with the aim to boost cellulose accessibility and reactivity. Among these methods, mechanical, chemical, enzymatic and thermal pretreatments[21] have been extensively practiced on both small lab as well as large industrial scales.

## 2.3 Cellulose solubility

Cellulose can neither melt when heated nor dissolve in the most common aqueous and organic solvents due to high DP and extensive intermolecular interactions, including both H-bonds and hydrophobic interactions stabilizing a semi-crystalline supramolecular and complex morphological organization. The former causes a decrease in entropy gain and the latter leads to poor enthalpy contribution.

# 3 Cellulose solvents

Cellulose solvents are specially composed systems that can be categorized as derivatizing and non-derivatizing media. It is noteworthy that there are some agents, which can swell cellulose to a certain extent but not dissolve it. These agents can be suitable as functionalisation media.

## 3.1 Derivatizing solvents

In derivatizing solvents, a cellulose derivative is formed, which is soluble in the reaction medium. These solvents can be used to regenerate cellulose fibres for applications for example in textiles, or the dissolved cellulose derivative can be further modified to yield necessary end products[22] such as carboxylic acid esters[23]. Examples of these solvents and the derivatives formed are as follows: $N_2O_4$/DMF (cellulose nitrite), $F_3CCOOH$ (cellulose trifluoroacetate), paraformaldehyde/DMSO (hydroxymethyl cellulose) and $ClSi(CH_3)_3$ (trimethylsilyl cellulose ether). Usually, the solubilizing substitution sits preferably at position 6 of AGU, which can later act as a protecting group for the subsequent derivatization. Next, during the workup process, an inverse functionalisation takes place and the solubilizing substitution is removed in an aqueous solution[24].

The most well-known derivatizing solvent for cellulose is $CS_2$/NaOH(aq), which is one of the oldest processing technologies pertaining to cellulose used in the viscose process. During this process alkali cellulose is treated with carbon disulfide ($CS_2$) and converted to cellulose xanthate (figure 4), which is soluble in dilute NaOH(aq)[25]. The yielded solution is called viscose, which is then forced into a spinneret in a sulfuric acid bath where xanthate ester is hydrolyzed, cellulose is regenerated and then spun into fibres for application in textiles. Approximately 6 million tons of cellulosic fibres are produced annually solely for use in the textile industry, with an estimated annual growth of 8% until 2025[26]. The viscose process is not only used to produce fibres, but also to convert the polymer into sponges and chest-like forms[27].

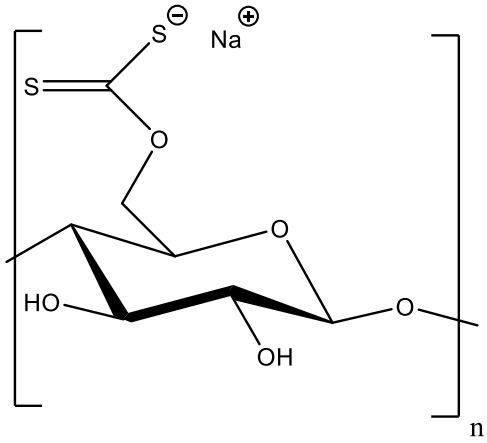


*Figure 4. cellulose xanthate*

## 3.2 Non-derivatizing solvents

In non-derivatizing solvents no cellulose derivative is formed, instead intermolecular interactions between the solvent and cellulose lead to the dissolution.

### 3.2.1 *N*-methylmorpholine *N*-oxide (NMMO)

Potential of NMMO to dissolve cellulose was first discovered and patented in 1970[28]. Currently, on an industrial scale, the Lyocell process uses NMMO for direct dissolution of cellulose mostly for textile fibre making purposes. Dilute solutions of NMMO(aq) only cause swelling in cellulose, while its monohydrate form (with 16% or less water content)[29] is able to dissolve high DP cellulose at temperatures above 80 °C[30]. After dissolution, a dry jet-wet spinning process is used where the dope is extruded out from the spinning nozzle and then into an air gap. Cellulose dissolution in NMMO occurs via hydrogen bond breakage specifically at O6, and establishment of both hydrogen bonds and ionic interactions between cellulose and NMMO[31–33] (figure 5). However, the main disadvantages of NMMO are its narrow temperature window and its instability at high temperatures, especially at water content below the monohydrate composition in the presence of heavy metal ions, charcoal and polyelectrolytes[33–36]. NMMO monohydrate has a melting point of 78 °C, while at temperatures higher than 120 °C, cellulose solutions are prone to strongly exothermic reactions and consequently sever degradation[33].

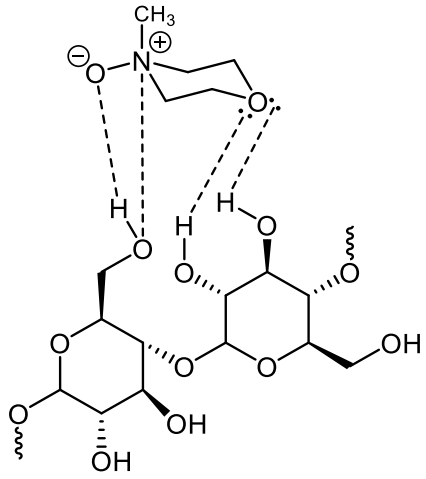

*Figure 5. NMMO-cellulose interaction, adapted from Sayyed et al.*[37]

### 3.2.2 Ionic liquids (ILs)

Ionic liquids are another class of solvents, which consist of organic cations and inorganic or organic anions able to dissolve cellulose. The first study on cellulose dissolution in ILs dates back to 1934 using *N*-alkylpyridinium chloride[38]. Most of the extensively studied ILs capable of dissolving cellulose have melting points below 100 °C. The advantages of using these solvents are low toxicity, low vapor pressure, and high thermal stability. Some of the commonly used ILs are composed of pyridinium, imidazolium, ammonium and phosphonium as cations and acetate ($OAc^-$), formate ($HCOO^-$), dimethyl phosphate $(MeO)_2 PO_2^-$ and chloride ($Cl^-$) as anions. In 2002, two well-known ILs—1-allyl-3-methylimidazolium chloride (AmimCl) and 1-ethyl-3-methylimidazolium acetate (EmimAc)—were found to be powerful cellulose solvents, which are able to dissolve up to 30 wt% cellulose with a high DP of 650 in only 30 mins[39]. Since then several research groups have investigated other ILs including imidazolium based ILs with varying anions (reporting efficient cellulose dissolution at room temperature)[40–43] and less toxic morpholinium based ILs for instance 4-allyl-4-methylmorpholinium acetate ([AMMorp]OAc), which could dissolve cellulose with a DP of 789 to a 30 wt% concentration at 120 °C in 20 minutes[44]. Studies regarding the mechanism of dissolution in ILs have shown that both the anion and cation contribute to the dissolution[45,46]. Overall, studies[47–49] have reported that anions disrupt the cellulose hydrogen bonds by forming hydrogen bonds with hydrogen of the cellulose hydroxyl groups, however the role of the cation is still being debated. The structure of a few cations in ILs are shown in figure 6.

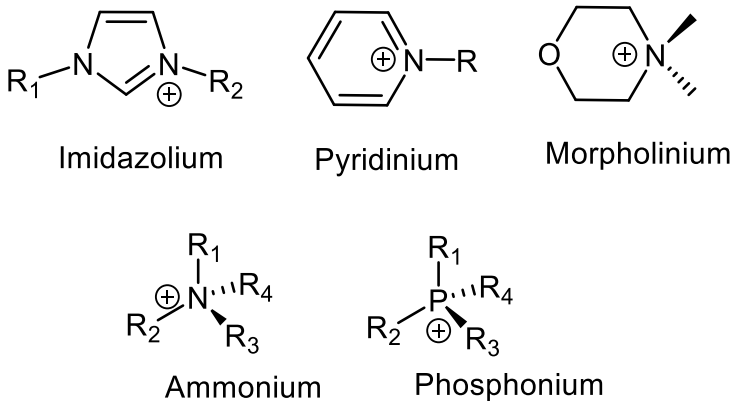


*Figure 6. Some cation structures in ILs*

## 3.3 Aqueous based solvents

### 3.3.1 Aqueous metal complexes

Among the oldest non-derivatizing solvents for cellulose, aqueous metal complexes have been known since 1857 when $Cu(OH)_2/NH_3$ (Cuam, Schweizer reagent) was first discovered. This solvent creates a strong complex with hydroxyl groups of cellulose at C2 and C3 (figure 7) and is still widely used for determination of cellulose DP through viscometry. Other metal complex solvents include $[Cu(H_2N\text{-}(CH_2)_2\text{-}NH_2)_2](OH)_2$ (Cuen), $[Cd(H_2N\text{–}(CH_2)_2\text{–}NH_2)_3](OH)_2$ (Cadoxen), Nitren, $[Ni(tren)(OH)_2]$ (tren = tris (2-aminoethyl)amine) and $[Pd(II)(\ H_2N\text{-}(CH_2)_2\text{-}NH_2)](OH)_2$[50–53].

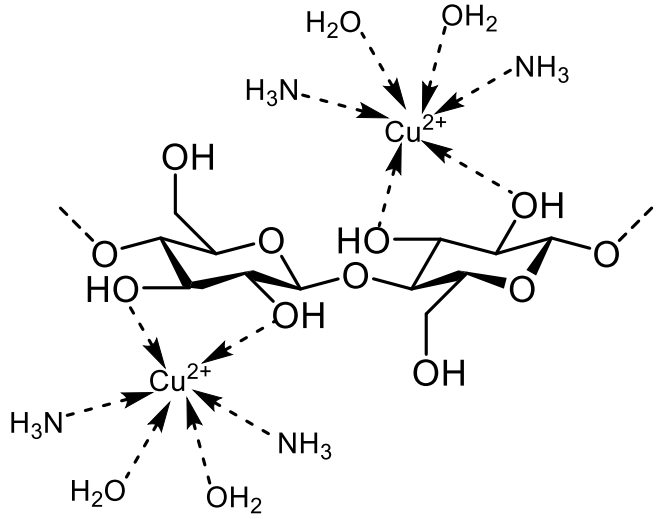


*Figure 7. Cuam– cellulose complex structure, illustrated by Wurm et al*[54].

### 3.3.2 Aqueous alkali hydroxides

Since 1928 several aqueous alkali hydroxides have shown the potential to swell and dissolve cellulose to a certain extent[55] for instance NaOH(aq), LiOH(aq), quaternary ammonium hydroxides (QAHs) and phosphonium hydroxides. This class of solvents is

gaining more attention due to their sustainability and applicability in large scales, in particular NaOH(aq) that has been extensively studied since the 1930s. It is able to either swell or dissolve cellulose depending on the temperature of dissolution, DP of cellulose and concentration of NaOH(aq). Sobue et.al. showed already in 1939 that NaOH(aq) at a concentration range between 7-10 wt% at -5 to +1 °C is able to dissolve cellulose[56]. Since then, a lot of efforts have been dedicated to study cellulose dissolution in NaOH(aq) by varying the dissolution conditions some of which could achieve dissolution of 5 wt % cellulose with DP of up to 200 in 9–10 wt% NaOH(aq) at about 10 °C. However, recent reports disclose the optimal conditions to be NaOH 8–9% wt% via freezing at –20 °C and subsequent thawing at room temperature. Since cellulose dissolved in NaOH(aq) is not stable over time and tends to irreversibly gel, some additives have been used to both aid the dissolution and delay the gelation. Overall, NaOH is considered to be a poor solvent since it is not able to dissolve cellulose with high DP, the maximum cellulose dissolution is low and the solutions are not stable over time requiring additives to aid dissolution and delay the commonly observed irreversible gelation[57]. Commonly used additives are ZnO[58], urea[59], thiourea[60] and polyethylene glycol (PEG)[61].

### 3.3.3 QAHs

Aqueous solutions of QAHs have been investigated as cellulose solvents since 1924[55] when a patent by Lilienfeld disclosed cellulose dissolution in 20-50 wt% solutions of tetraethylammonium hydroxide (TEAH), tetramethylammonium hydroxide (TMAH) and benzyltriemethylammonium hydroxide (Triton B) at room temperature (figure 8). Later it was discovered that benzyl-substituted QAHs are even more powerful solvents[62,63], namely Triton B and Triton F[64,65].

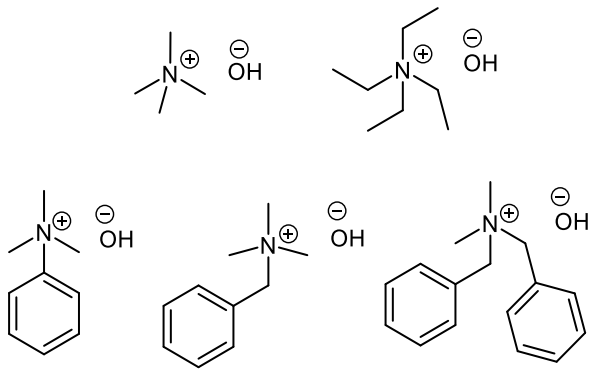


*Figure 8. Top row from left to right: TMAH, TEAH, bottom row from left to right: trimethylphenylammonium hydroxide, Triton B and Triton F*

Higher efficiency of QAHs containing benzyl groups, compared to alkyl groups (methyl, ethyl, propyl, and butyl) has been commonly attributed to the bulkiness of the cation. This possibly contributes to the interruption of cellulose-cellulose interactions and the

separation of the cellulose chains, effectively acting as a wedge[66]. Brownsette et.al.[65] investigated cellulose dissolution in different concentrations of Triton B at 20 °C and reported two maximum dissolutions (maximum amount of dissolved cellulose) at 20 °C: one at a lower concentration of 2.15 N and the other at 3.5 N. The second maximum solubility was also detected in TMAH and the concentration needed to obtain maximum solubility in NaOH, LiOH and TMAH were 3 N, 3.3 N and 2.5 N, respectively. Besides, another finding disclosed a decrease in solvent concentration required for maximum cellulose solubility by decreasing the temperature to 0 °C. On the other hand, the same authors reported Triton F (containing an additional benzyl group compared to Triton B) as a better solvent compared to Triton B, TMAH, NaOH and LiOH since the first maximum solubility required a lower base concentration (1.9 N). Moreover, when cellulose is dissolved in Triton F it can be diluted to 0.5 N without any cellulose precipitation.

Among other QAHs, aqueous solutions of tetrabutylammonium hydroxide (TBAH) and alkylphosphonium hydroxide have also been reported to dissolve lignocellulosic materials[67–69]. In a recent study 40 wt% TBAH(aq) was able to dissolve cellulose and molecular dissolution was detected at lower concentrations, while cellulose aggregates could be detected at higher concentrations measured by static light and small-angle X-ray scattering[70]. According to another report, TBAH can dissolve up to 20 wt% microcrystalline cellulose (MCC)[71].

#### 3.3.3.1 Understanding dissolution mechanism in aqueous alkali

The dissolution mechanism of cellulose in aqueous alkaline media has not yet been fully understood. However, studies particularly those on cellulose in NaOH(aq), suggest that the dissolution takes place via the disruption of H-bonding by competitive intermolecular interaction between OH groups of the solvent and cellulose, which includes partial deprotonation. In addition, there is the possibility that the cation has a role in preventing the re-association of dissolved cellulose by distribution between individual chains[72]. In this regard, higher hydrophobicity of the cation has been reported to promote the dissolution and stability of the solution[73]. Thus, the role of the hydrophobic assembly effect and the amphiphilic structure of cellulose on its dissolution and stability of the dissolved state in aqueous systems[74] should also be considered.

# 4 Chemical modification

Chemical functionalisation is a way to modify cellulose properties and/or enhance its solubility. This can be done either heterogeneously or homogeneously. In the former the accessibility of the hydroxyl groups is the primary determining factor since the fibre structure is maintained while in the latter complete dissolution of cellulose is usually achieved and as a result all cellulose OH groups are assumed to be equally available. Currently, cellulose esters and ethers, the most common cellulose derivatives, are predominantly synthesised heterogeneously on an industrial scale, mainly due to poor solubility of cellulose in the most conventional solvents. However, heterogeneous synthesis of cellulose derivatives has some obvious limitations such as poor substitution control due to low accessibility of cellulose hydroxyl groups and poor control of substitution pattern. The most commonly produced derivatives, for instance carboxymethyl cellulose (CMC) and cellulose acetate (CA) (figure 9) are used as blends from several batches to adjust their properties[75]. In contrast, homogeneous cellulose modification has the advantages of improved control of substitution distribution and thus products properties, possibility of regioselective reactions and a better control of cellulose degradation[75,76].

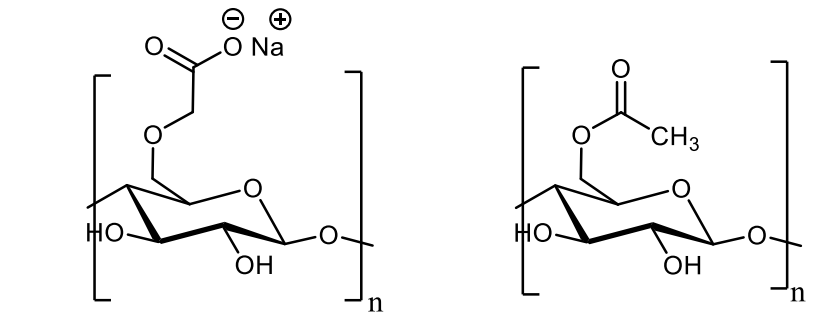


*Figure 9. Two most common cellulose derivatives*

## 4.1 Modification in *N,N*-Dimethylacetamide/Lithium Chloride (DMAc/LiCl)

DMAc/LiCl is the most commonly used aprotic solvent for homogeneous modification of cellulose. A pre-treatment step such as solvent exchange[75] or thermal heating[76] is

required prior to cellulose dissolution. Cellulose dissolution occurs when $Li^+$ $(DMAc)_x$ cationic complex is formed where $Li^+$ cations strongly couple with the carbonyl oxygen of DMAc and the free $Cl^-$ breaks the intermolecular H-bonds between cellulose chains forming new H-bonds to cellulose hydroxyl groups.

Several modifications have been carried out in DMAc/LiCl including esterification, etherification as well as grafting reactions. An example in which high DS of 2.25 was obtained, is the synthesis of cellulose succinate and cellulose phthalate under microwave heating in only 10 minutes in presence of some catalysts including 4-dimethylaminopyridine (DMAP) by Chadlia et al.[77] (figure 10).

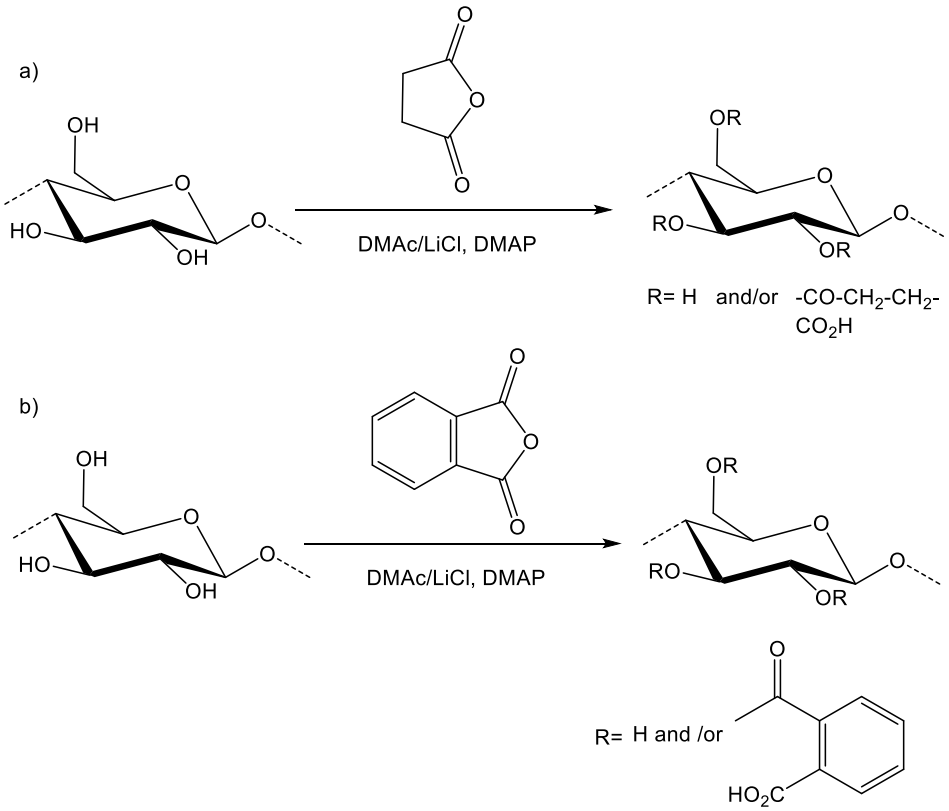


*Figure 10. Synthesis of a) cellulose succinate b) cellulose phthalate*

## 4.2 Cellulose modification in aqueous alkali hydroxides

There are very few studies on cellulose modification in aqueous bases being challenging mainly due to competing reactions with water and production of several by-products. Amongst the water-based solvents, aqueous NaOH/urea has been used in several attempts to modify cellulose chemically. For example, Zhou et al. synthesized hydroxypropyl cellulose (HPC) with DS=0.85 using propylene oxide and methyl cellulose (MC) with DS=1.48 using dimethyl sulfate[78]. Their $^{13}C$ NMR data showed a slightly higher substitution on C2 compared to C3 and C6. In another study, hydroxyethyl cellulose was synthesized using chlorohydrin with maximum DS of 1.14[79] and a slightly higher relative DS values on C2 and C6 compared to C3. In addition,

cellulose-based polyelectrolytes were synthesized using acrylamide[80]. In the first step cellulose was substituted with amide groups, which later underwent saponification to transform into carboxyl groups. These groups became charged in neutral as well as alkaline medium and showed polyelectrolyte properties (figure 11).

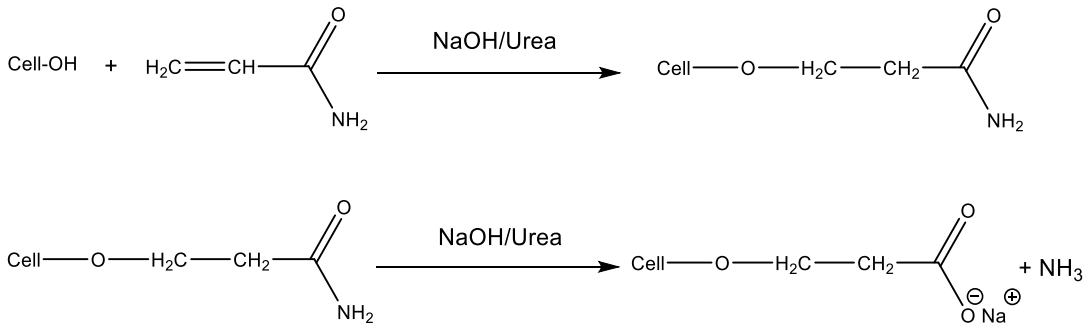


*Figure 11. synthesis of cellulose-based polyelectrolytes in NaOH/Urea*

Chemical cross-linking is another example of cellulose modification using epichlohydrine in aqueous NaOH/urea, which has been reported by several research groups[81–83]. Both heating to 50 °C and freezing were used to produce the cellulose gel, which was later coagulated in a water bath. The obtained cellulose gel was reported to be transparent, in contrast to the usual opaque coagulated cellulose. The transparency is attributed to the homogeneity when cellulose is cross-linked.

Though dissolution in aqueous quaternary ammonium hydroxides has been investigated widely, thus far there has only been one study regarding chemical modification in aqueous TEAOH[84]. The authors reported homogeneous etherification of microcrystalline cellulose with glycidyl trimethylammonium chloride (GTAC) in aqueous TEAOH-carbamide solvent (figure 12). The carbamides used were urea, methylurea, ethylurea, 1,3-dimethylurea and imidazolidone-urea, amongst which the highest modification yield was obtained when using 1,3-dimethylurea. The achieved yield was more than two times that of the yield of modification in NaOH/urea.

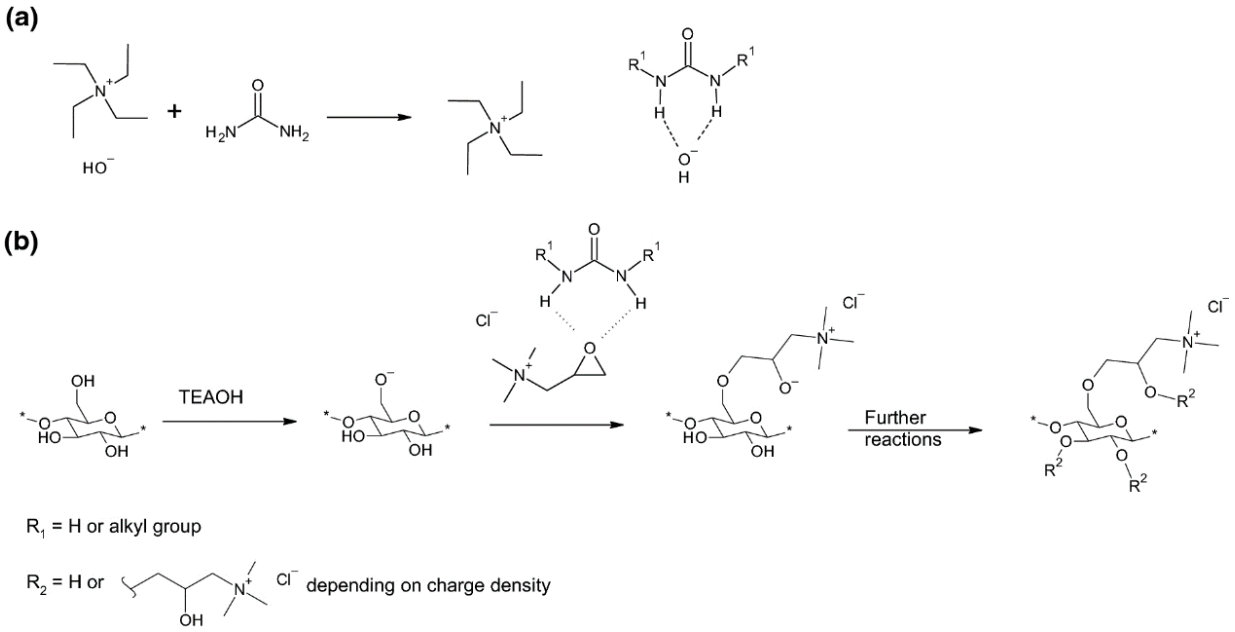


*Figure 12. Homogeneous etherification of cellulose in aqueous TEOAH-carbamide*[84]

Thus, it is evident that further efforts are needed towards understanding and improving homogeneous modification of cellulose in these media.

# 5 Materials and Methods

## 5.1 Materials

In the first study, microcrystalline cellulose (MCC), made by acid hydrolysis of specialty wood pulp -Avicel PH-101- with a degree of polymerization of 180, NaOH, benzyltrimethylammonium hydroxide (Triton B) 40 wt% in $H_2O$, tetramethylammonium hydroxide (TMAH, 25 wt% in $H_2O$) and allyl glycidyl ether (AGE) were purchased from Sigma-Aldrich and used as received.

In the second study, a prehydrolysis kraft dissolving grade hardwood pulp from Eucalypt and a sulfite dissolving grade pulp from softwood with viscosities 283 $cm^3/g$ and 442 $cm^3/g$ were provided by Bracell and Domsjö respectively. In addition, *N*-methyl morpholine, Iodomethane were purchased from Merck and silver oxide was purchased from Alfa Aesar.
More details can be found in the appended papers.

## 5.2 Methods

### 5.2.1 Dissolution of microcrystalline cellulose and pulp

Dissolution of cellulose was carried out using the freeze-thaw method. In Paper I, a desired concentration of the base was prepared by the addition of deionized water and then MCC was added to the solvent to reach a final concentration of 3 wt%. The suspension was stirred in an ice bath until most of the cellulose was dissolved. Then the solutions were kept at -25 °C for 20 minutes and thawed afterwards.

In Paper II a set of base concentrations were prepared by addition of deionized water. Next, a desired amount of MCC was added to the solvents to reach the final concentration of 3 wt%. The suspension was stirred for 5 minutes to ensure it was well-dispersed and kept at -25 °C for 20 minutes and thawed afterwards.

### 5.2.2 Etherification of microcrystalline cellulose

AGE was added to the prepared cellulose solutions at the ratio of 3 mol AGE: 1 mol OH of cellulose. The solutions were stirred at 50 °C for 2 hours under $N_2$. After the

reaction completion ethanol was added to allow the product to diffuse out of the solution, dialyzed against deionized water for 1 week and finally freeze-dried.

## 5.3 Characterization

### 5.3.1 *In-situ* IR spectroscopy and *in-situ* Rheology measurements

In order to follow the reaction in real time and gain a deeper insight on the kinetics of etherification and the associated side reaction (AGE hydrolysis), *in-situ* IR spectroscopy was used. In this method, a probe with a gold sealed diamond tip was immersed in the solutions for 2 hours. *In-situ* rheology measurements were used as a complement here to assess the homogeneity and stability of the solutions during the course of reaction and investigate whether the end of the reaction could be detected. For this study, steady share measurements using a double gap cylinder was applied and the measurements were run for 1 hour.

### 5.3.2 ATR-FTIR

To characterize the yielded cellulose ether, the products were examined on a PerkinElmer Frontier equipped with Attenuated total reflectance (ATR) sampling accessory and spectra in a transmittance mode with a resolution of 4 $cm^{-1}$ and 20 scans were collected.

### 5.3.3 NMR spectroscopy

In Paper I, $^{1}H$ NMR, quantitative $^{13}C$ NMR and HSQC spectra were collected to confirm the product formation, assign the product peaks, and analyze the molar substitution (MS). All of the spectra were collected at 25 °C on a Bruker AVANCE III HD 18.8 T NMR spectrometer, equipped with a 5 mm TXO Cryoprobe and operating at a frequency of 800 MHz for $^{1}H$ and 201 MHz for $^{13}C$.

In Paper II, to confirm NDMM-OH synthesis, $^{1}H$ NMR and $^{13}C$ NMR spectra were recorded in $D_2O$ at 25 °C using a Varian (400-MHz) spectrometer equipped with One NMR Probe. In addition, to confirm chemical stability of cellulose solutions in NDMM-OH(aq) and investigate whether any extra peaks could be detected, $^{13}C$ NMR experiments were carried out in $D_2O$ on an 800 MHz ($^{1}H$) magnet with a TXO probe and Bruker Avance HDIII console using a z-restored spin echo sequence to avoid a rolling baseline.

### 5.3.4 Microscopy

To detect the undissolved material in cellulose solutions, a microscope (ZEISS SteREO Discovery.V12) equipped with a camera at ambient temperature was used. When no particles could be observed the dissolution was confirmed. In addition, UV-Vis measurements were used as a complementary study to confirm dissolution.

### 5.3.5 UV-Visible measurements

To assess the turbidity as indicative of the dissolution state of cellulose and complement the microscopy investigations, the transmittance of the light was measured through solutions using a double-beam spectrometer (Specord 205) with a spectral bandwidth of 1.4 nm was used.

### 5.3.6 Size exclusion chromatography (SEC)

In Paper II, SEC was used to detect possible degradation, evaluate the stability of cellulose dissolved in NDMM-OH(aq) and investigate its molecular weight distribution. These measurements were run by a chromatography system from Polymer Laboratories, comprised of a PL-GPC 220 with an RI detector.

### 5.3.7 Intrinsic viscosity

A good solvent causes cellulose chain extension. Therefore, in Paper II to evaluate the quality of the solvent, intrinsic viscosity measurements using a capillary viscometer (equipped with circulating water bath to maintain the temperature at 25 °C) were carried out.

### 5.3.8 Dynamic light scattering (DLS)

In a good solvent, cellulose is usually molecularly dissolved. To investigate this, DLS studies on both unfiltered and filtered solutions were performed and the hydrodynamic radius of the cellulose at a dilute concentration was measured. A Zetasizer Nano ZS from Malvern Panalytical, with a 4 mW 632.8 nm red laser at a scattering angle of 175° at 20 °C, was used for the measurements

# 6 Results and discussion

## 6.1 Probing the impact of the hydroxide base composition on cellulose etherification

The potential of aqueous Triton B, TMAH and NaOH, both individually and in combinations as cellulose solvents has been investigated in previous works by our group[85,86]. Thus, to perform a comprehensive study on cellulose modification in these bases, the objectives of the first study were set on developing methods to monitor cellulose etherification and addressing its challenges and assets, as well as gaining a deeper understanding of the impact of solvent composition on cellulose reactivity and stability. Thus, cellulose etherification using allyl glycidyl ether (AGE) in the aforementioned solvents was selected as the model reaction for further investigations. Structures of Triton B and TMAH as well as the model etherification reaction in this study are shown in scheme 1.

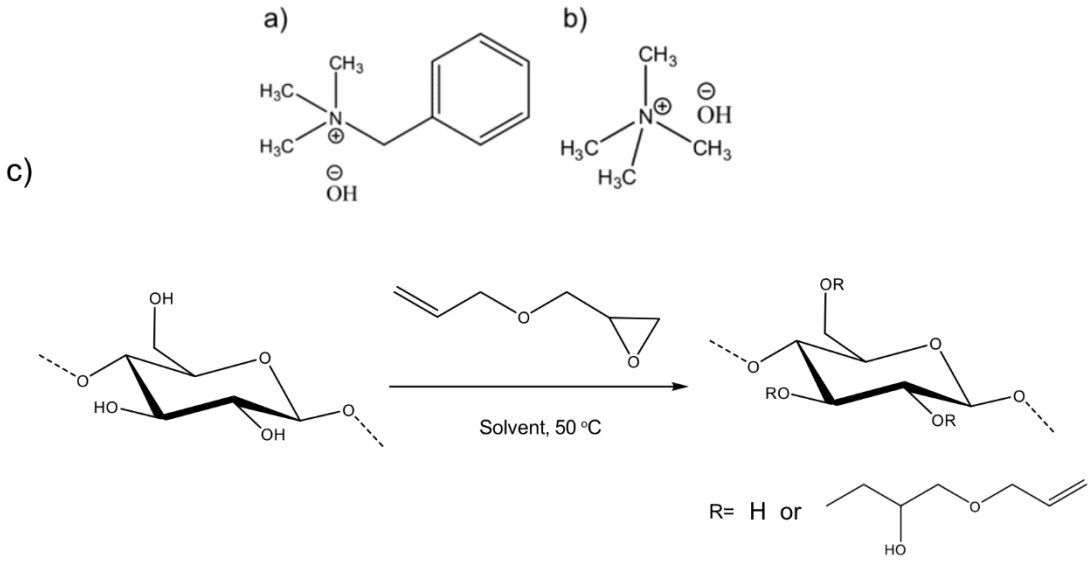


*Scheme 1. a) Triton B b) TMAH c) model etherification reaction*

### 6.1.1 Monitoring of cellulose etherification by *in-situ* IR spectroscopy

Performing kinetic studies on cellulose etherification in water-based solutions is quite challenging due to the occurrence of side reactions including hydrolysis of the reagent and self-etherification of the reagent (referred to as a cascade reaction). In addition, there are multiple overlaps of the peaks from side-products, solvents, and cellulose. However, valuable information can be extracted aiding the comparison between etherification in different reaction media.

In the initial study, all the reactions were carried out for 2h under $N_2$ (to exclude interference of $CO_2$ from air with the IR spectra) and with reflux (to exclude variations due to water evaporation), monitored by *in-situ* IR spectroscopy. Figure 13 shows the overview of cellulose etherification in Triton B. This figure shows spectra collected at a specific time interval in different colors as the reaction progresses.

As it can be seen, the main change in the IR absorption bands is detected to be in the region between 900-1100 $cm^{-1}$, which contains information on both cellulose etherification and hydrolysis of AGE. Furthermore, a minor decrease in the water peak at 1640 $cm^{-1}$ and the carbonate peak at 1480 $cm^{-1}$ can be detected because of a small water loss and most likely elimination of atmospheric $CO_2$ when performing the reaction under $N_2$ respectively[87].

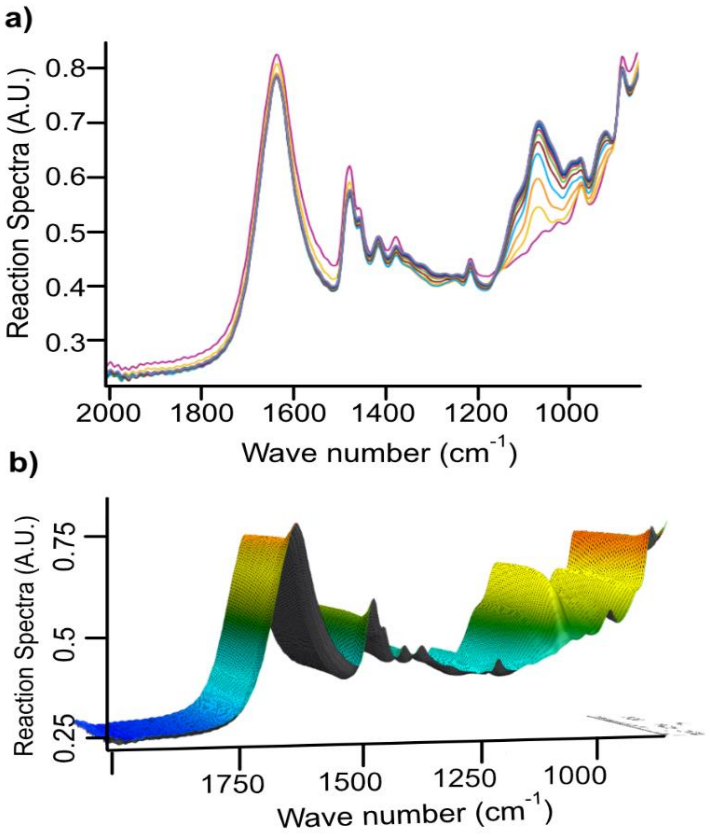


*Figure 13. a) Overview of the reaction in Triton B, and b) its corresponding 3D plot*

In an initial effort to determine distinct peaks to follow, AGE as well as AGE in aqueous Triton B reference spectra were collected and superimposed as shown in figure 14. As in this figure and since AGE does not dissolve in these aqueous bases immediately (a biphasic solution is formed upon addition of AGE to the selected solvents followed by complete dissolution after a while), one possible analysis is to follow oxirane ring peak in AGE (as it is exposed to ring opening in etherification reaction) to monitor its dissolution and later consumption during the course of reaction. Thus, the peak at 1253 $cm^{-1}$ (circled in figure 14) was selected and its corresponding trends during the reaction time in different solvents were compiled in figure 15.

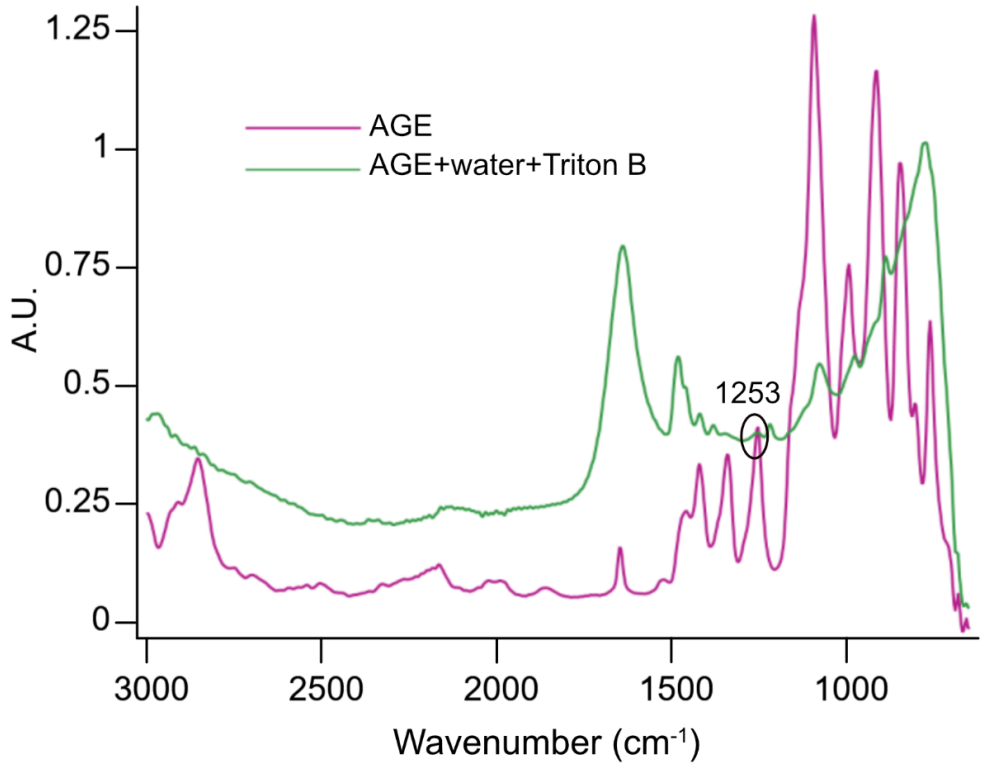


*Figure 14. Pure AGE and AGE/aqueous Triton B spectra*

All the trends show an initial increase interpreted as AGE dissolution, followed by a decrease due to its consumption in the reaction and finally a plateau when no more changes take place. All the reaction media show similar rates except for NaOH, which clearly takes a much longer time to dissolve and later be consumed.

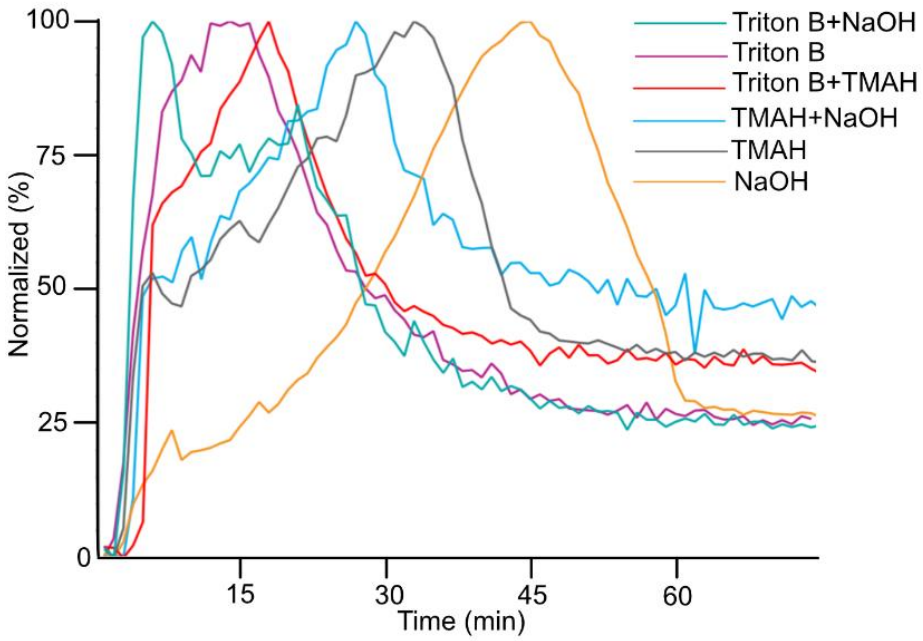


*Figure 15. Peak at 1253 cm$^{-1}$ in different bases*

In another attempt, the region between 900-1100 cm$^{-1}$, which reflects some key chemical conversions, was subjected to further analysis. The overview of the spectra changes in this region during the reactions is shown in figure 16. During etherification of cellulose usually the height of the peaks increases up to a certain point after which the spectra remain unchanged. A careful look at this figure discloses that a decrease in intensity of the trends in NaOH (figure 16a) can be detected after reaching its maximum. The same behavior but to a much less extent could be observed in TMAH/NaOH (figure 16e). This behavior is due to lower temperature stability of cellulose solution in NaOH(aq) causing cellulose precipitation resulting in its disappearance from the IR probe, thus a decrease in the height of the peaks. The same reason is valid for cellulose solution in TMAH/NaOH(aq) but to a much less pronounced degree. However, no decrease in peak height is detected in other solutions, which is an indicative of their higher temperature stability. It is notable that, compared to cellulose solution in NaOH(aq), which became cloudy and turbid shortly after the reaction started in the oil bath (at 50 °C), cellulose solutions in other bases remained transparent.

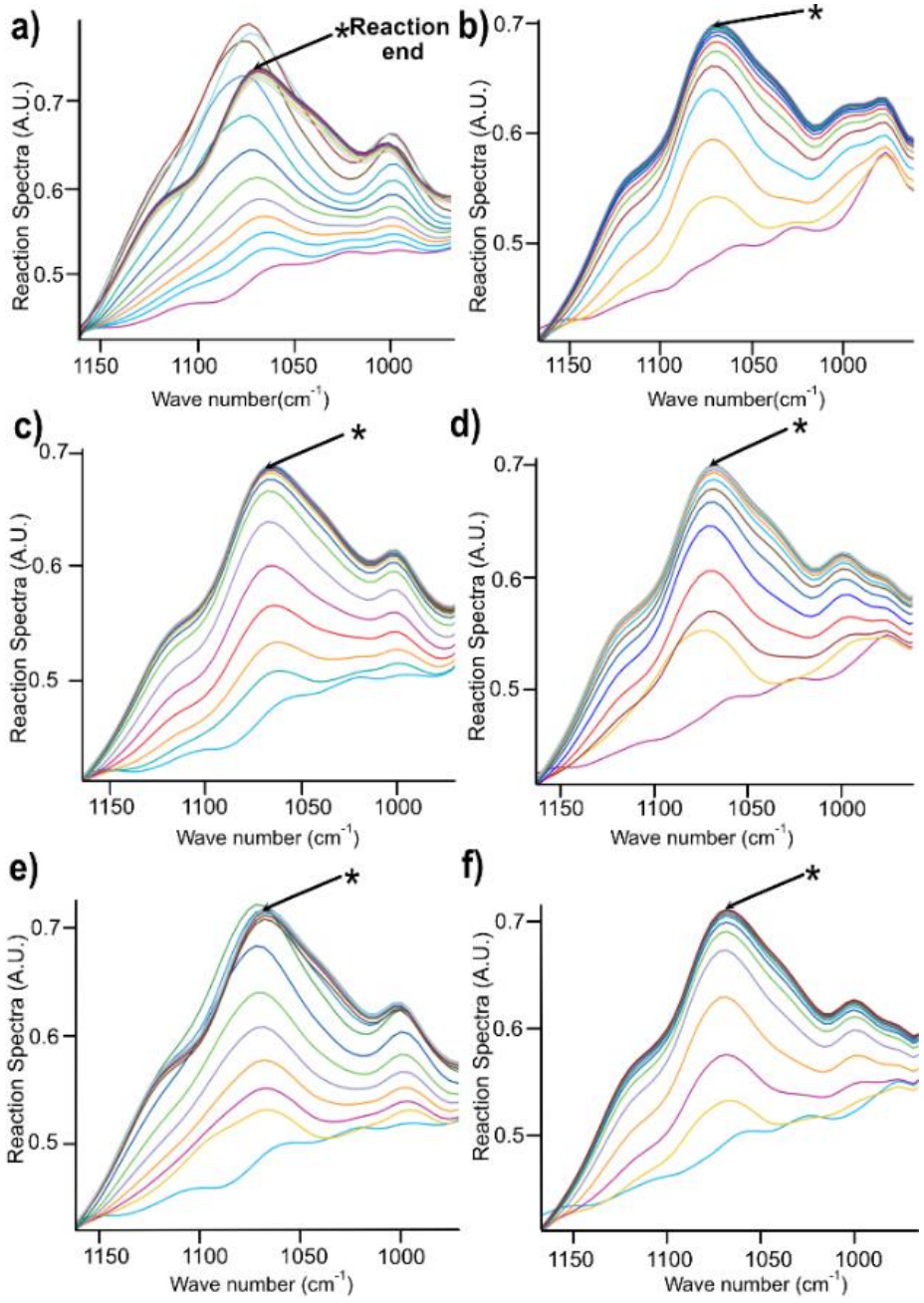


*Figure 16. Changes in the region between 900-1100 cm $^{-1}$ during the course of reaction in a) NaOH b) Triton B c) TMAH d) Triton B/NaOH e) TMAH/NaOH f) TMAH/Triton B*

One challenge with analysis in this region was that it is comprised of different types of C-O- moieties originating from both etherification and hydrolysis, which extensively overlapped with each other. To aid analysis of the spectra and assign peaks to cellulose, AGE, 3-allyloxy-2-hydroxypropyl-cellulose (AHP-cellulose, the product of cellulose etherification) and diol, relevant reference spectra were collected and superimposed in figure 17a. In addition, etherification of MCC was monitored while adding AGE in several aliquots in order to enable easier identification of absorption bands relevant to etherification/reagent consumption (figure 17c). This allowed us to monitor even minor changes in spectra while adding the reagent stepwise. Besides, since AGE hydrolysis is

a side reaction, in another reference experiment, AGE was allowed to react in absence of MCC (figure 17d) to monitor its hydrolysis, distinguish differences in spectra overview with and without cellulose and identify any peaks unique to hydrolysis.

Careful analysis of the obtained spectra (figure 17a) led to a distinction of two different peaks at 996 $cm^{-1}$ and 1028 $cm^{-1}$. The peak at 996 $cm^{-1}$ is indicative of AGE hydrolysis since it is present only in the AGE hydrolysis spectra. It also showed continuous increase followed by a plateau during reference hydrolysis reaction (figure 17b) as well as in etherification (figure 18). The peak at 1028 $cm^{-1}$ was detected in both cellulose and AHP-cellulose, which is indicative of C-O moieties arising from different compounds (e.g., hemiacetals and acetals from the cellulose backbone and ether bonds from the introduced substituents in the AHP-cellulose). Subsequent comparison analysis between figure 17c and 17d showed that the peak at 1028 $cm^{-1}$ continuously increased in both etherification and AGE hydrolysis. Besides, no other distinct peaks could unfortunately be detected making it impossible to isolate a peak corresponding to etherification with no contribution of hydrolysis. Consequently, the only possible peak to monitor was 996 $cm^{-1}$.

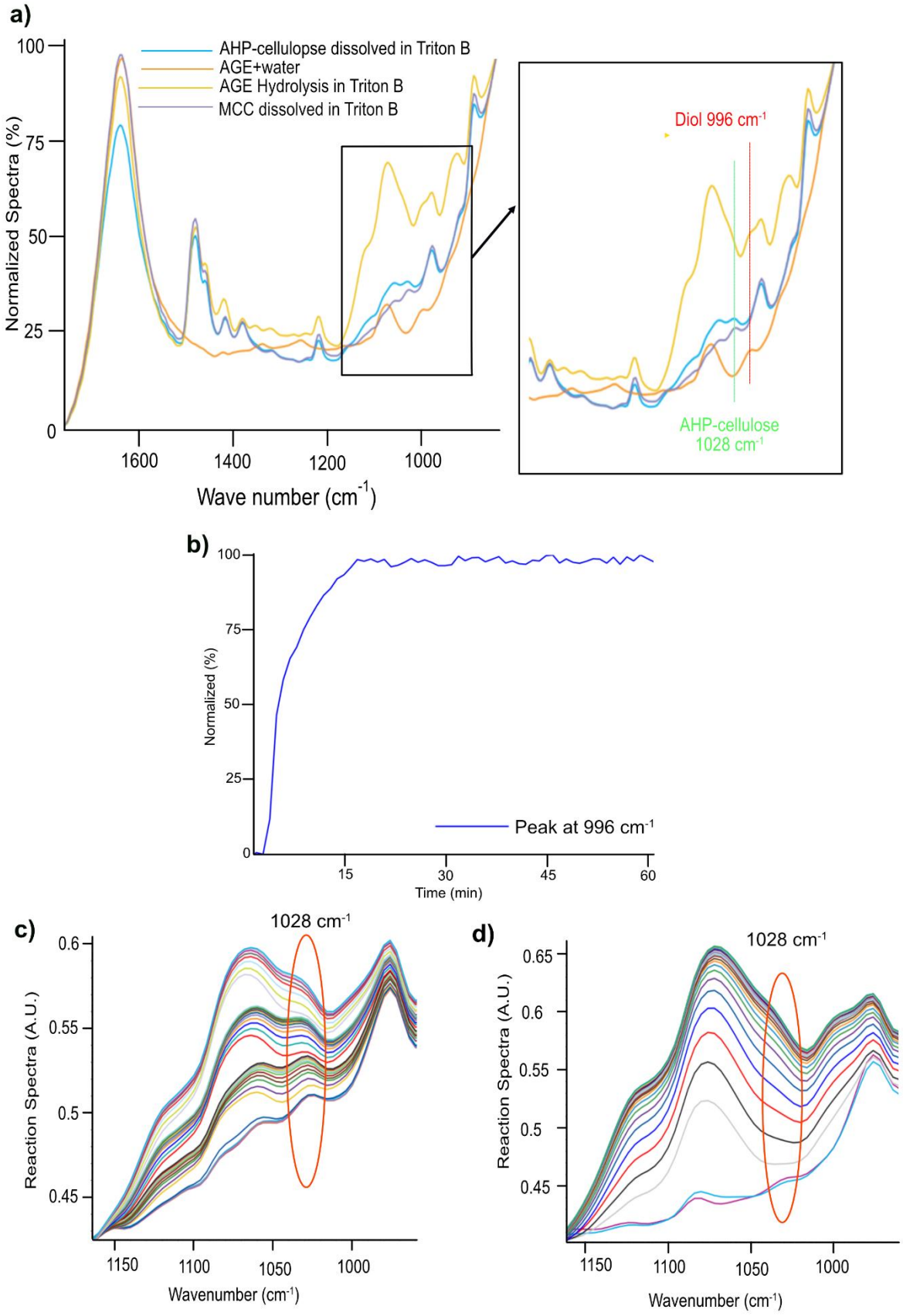


*Figure 17. a) Spectra comparison for peak assignment b) Peak at 996 cm-1 in AGE hydrolysis in absence of MCC (in Triton B) c) MCC etherification by AGE addition in aliquots in Triton B d) AGE hydrolysis in Triton B*

To investigate the deviation of the peak trends at 996 $cm^{-1}$ in different reaction media, their traces from each base were compiled as presented in figure 18. A comparison between the trends reveals very similar behaviour in which NaOH has the slowest hydrolysis while these peaks in Triton B/TMAH take the shortest time to reach their maximum. These are most likely as a result of faster AGE dissolution in other reaction media compared to NaOH.

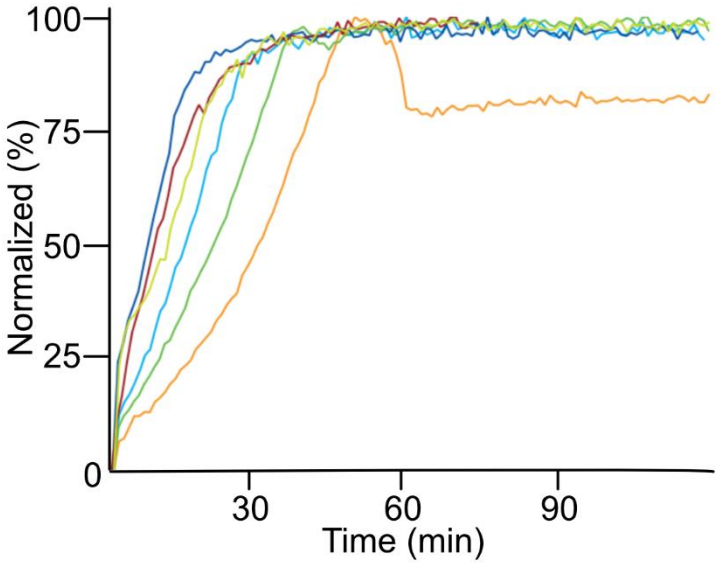


*Figure 18. Comparison of the peak at 996 $cm^{-1}$ in different bases.*

The end points of the experiments (when no more etherification and hydrolysis can be detected) were estimated as the time after which the absorption in the C-O region remained unchanged and the results are summarized in table 1. According to the results, Triton B as well as TMAH/Triton B had similar reaction times and took the least time for the reaction to reach its equilibrium. It seems that addition of TMAH to Triton B does not enhance the kinetics of the reaction, however, the reasons remain to be investigated. The reactions took relatively longer time in other solvents and in case of NaOH cellulose started to precipitate after 46 minutes.

*Table 1. Etherification of cellulose in different aqueous hydroxide solvents*

| Solvent | Reagent consumption time (min) |
|---|---|
| NaOH | 46 (precipitation time) |
| Triton B | 28 |
| TMAH | 35 |
| Triton B/NaOH | 46 |
| TMAH/NaOH | 47 |
| Triton B/TMAH | 27 |

### 6.1.2 *In-situ* Rheology measurements

These measurements were run as a complement to *in-situ* IR spectroscopy experiments and to investigate whether homogeneity and end points of the reactions could be detected. Figure 19 displays the reduced transient viscosity ($\eta^+/\eta_0$), in which $\eta^+(t)$ is the instantaneous transient viscosity and $\eta_0$ is the viscosity at t=0, vs. time. All the experiments were run for 1h at constant shear rate, $\dot{\gamma} = 1500$ 1/s. When performing *in-situ* IR spectroscopy measurement the solutions were stirred vigorously, thus, to keep the reaction conditions as constant as possible the aforementioned high shear-rate was selected ($\dot{\gamma} = 1500$ 1/s being the maximum rate possible in the applied rheometer). All the systems showed a similar initial decrease in viscosity due to AGE addition, which caused a dilution in the system followed by an increase in viscosity as a result of reaction progression (probably due to formation of AHP-cellulose with a higher molecular weight compound). It should be noted that viscosity change was not extensive, however, when Triton B was used either alone or in combinations, smooth viscosity curves were obtained, and the fastest viscosity increase was detected after 40 min followed by a plateau. *In-situ* IR spectroscopy results have shown that after 28 mins the reaction stopped in Triton B (table 1). The fact that longer time was detected for reaction completion in steady-shear measurements indicates that the mixing rate was lower compared to when the reactions were *in-situ* monitored. However, significant distortions were observed in NaOH and TMAH, which were most likely due to inhomogeneities that were formed as a result of the less optimal mixing conditions. These cellulose aggregates travelled up in the measuring cylinder and interrupted the measurements, consequently, appearing as jumps in the curves. Except for NaOH, all other curves almost reached the maximum viscosity while NaOH (figure 19c) still showed an ongoing viscosity increase confirming less temperature stability. Hence, *in-situ* rheology measurements have proven to be a valuable tool in assessing the homogeneity (thermal stability) of the solutions and aiding with reaction end determination provided that similar mixing conditions are provided.

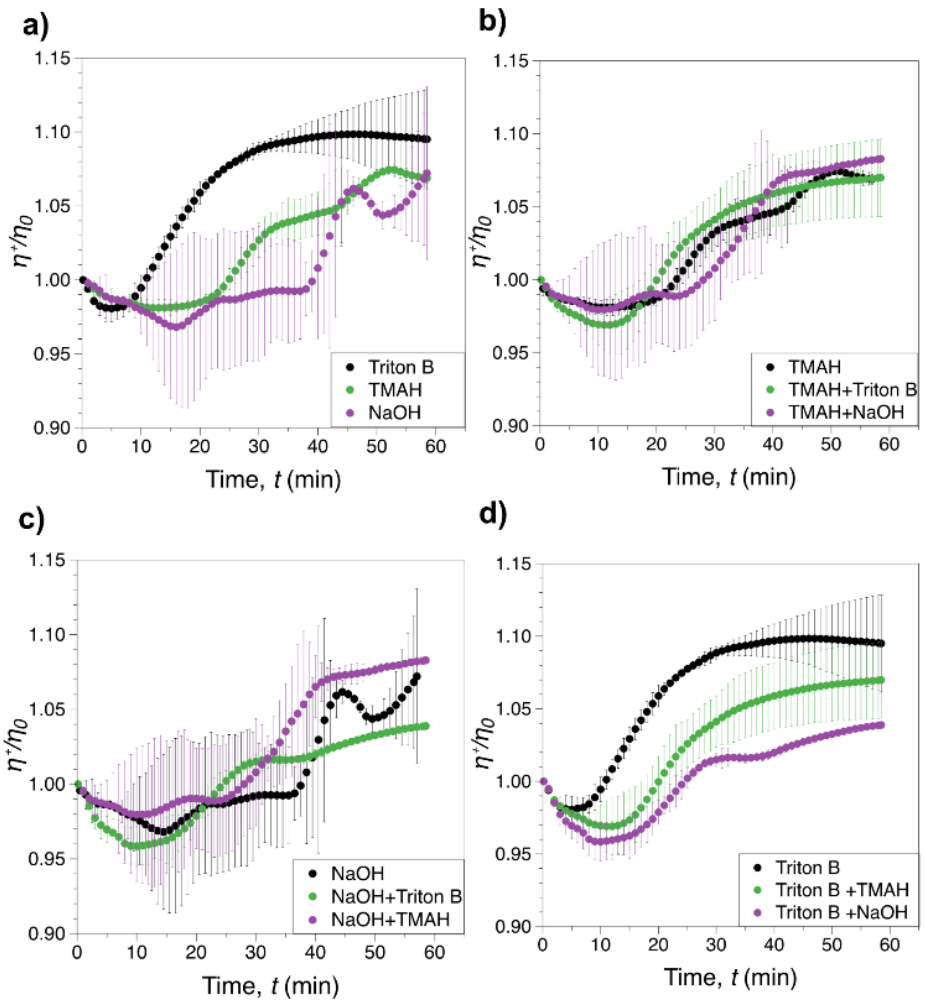


*Figure 19. Reduced transient viscosity, $\eta^+/\eta_0$, where $\eta^+(t)$- is the instantaneous transient viscosity and $\eta_0$ is the viscosity at t=0, vs. time at constant shear rate, $\dot{\gamma} = 1500$ 1/s for: a) individual solvents, b) TMAH and its combinations with other bases, c) NaOH and its combinations with other bases and d) Triton B and its combinations with other bases. The error bars represent the standard deviation based on averaging 2 individual measurements.*

### 6.1.3 ATR-FTIR

Figure 20 shows ATR-FTIR spectra of unmodified cellulose and 3-allyloxy-2-hydroxypropyl-cellulose (AHP-cellulose) yielded in NaOH, Triton B, TMAH as well as mixtures of the mentioned bases. This characterization was used only as a qualitative mean to confirm AHP-cellulose synthesis. All the spectra show a noticeable increase in the peak at 1646 $cm^{-1}$ assigned to C=C. Furthermore, four distinct shoulders appeared at approximately 930 $cm^{-1}$, 1060 $cm^{-1}$, 1422 $cm^{-1}$ and 2876 $cm^{-1}$ assigned to $=CH_2$, C-O-C, $CH_2$ scissoring and C-H respectively[88,89]. In comparison with MCC, aforementioned peaks showed a remarkable increase.

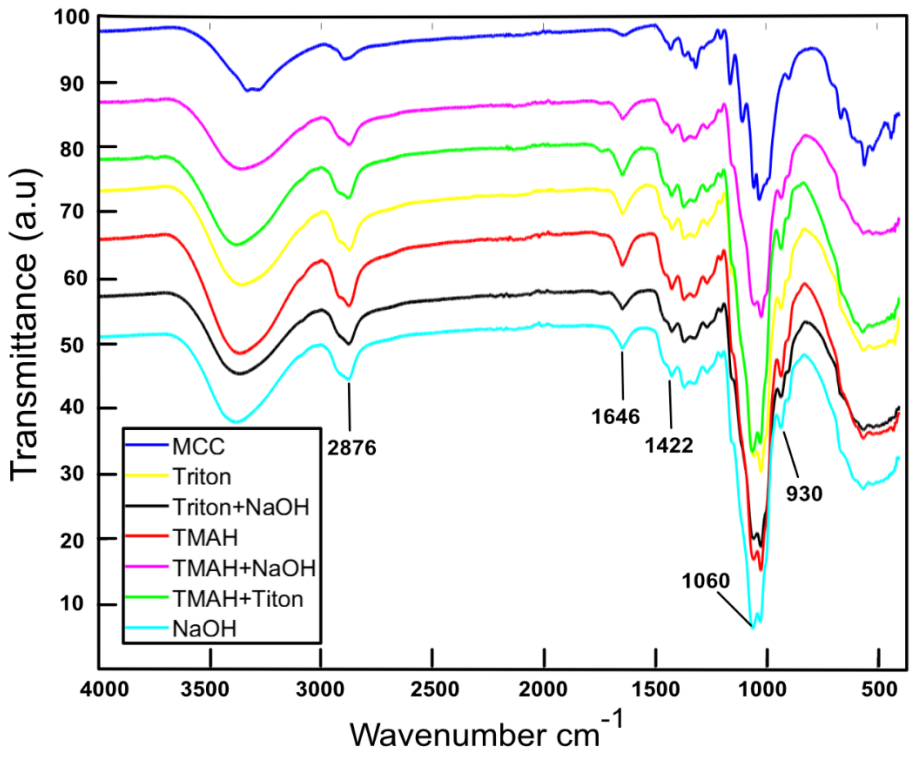


*Figure 20. comparative ATR-FTIR spectra of MCC and AHP-cellulose synthesized in different alkaline solutions*

### 6.1.4 NMR characterization and estimation of the molar substitution (MS)

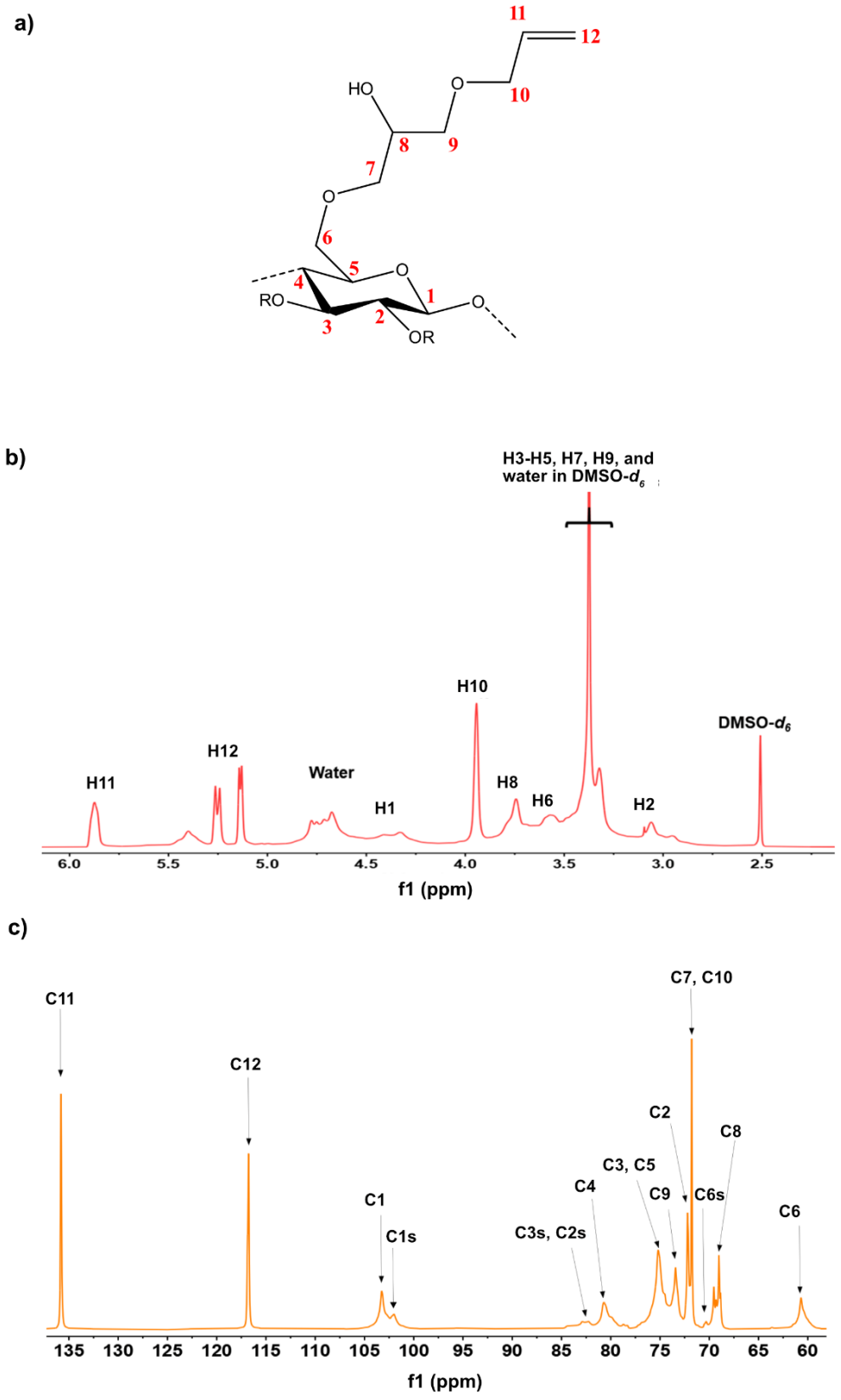


*Figure 21. AHP-cellulose synthesized in TMAH a) structure b) $^{1}H$ NMR and c) $^{13}C$ NMR spectrum*

Synthesis of AHP-cellulose (figure 21a) was confirmed by both $^{1}H$ NMR and quantitative $^{13}C$ NMR (figure 21b and 21c). As shown in figure 21b, the signal at 3.06 was assigned to H2 of AGU and the broader peak in 3.0-3.50 was attributed to 5 similar magnetic protons including H3-H5 of AGU, H7 and H9 of AGE substitution. The signal at 3.9 is assigned to two protons labelled as H10, the singlet signal at 3.6 is attributed to H8 and the singlet peak at 3.5 is characteristic of H6. The peak at 4.3 ppm corresponds to alpha anomeric H1 of AGU, which appears at a higher shift due to two neighboring oxygen atoms. Finally, the peaks at 5.8 and 5.2 are assigned to methine proton of AGE (H11) and 2 protons of H12, respectively.

Figure 21c is the $^{13}C$ NMR of AHP-cellulose obtained in TMAH, which shows the partial substitution on all cellulose hydroxyl groups at 70.5, 82.25, 82.89 and 102.02 ppm attributed to substituted C6, C2, C3, and C1s respectively. In addition, C1 shows an additional peak at 102 ppm due to the substitution of its adjacent carbon (C2). These results were confirmed by HSQC analysis for all the studied solvents (figure 22).

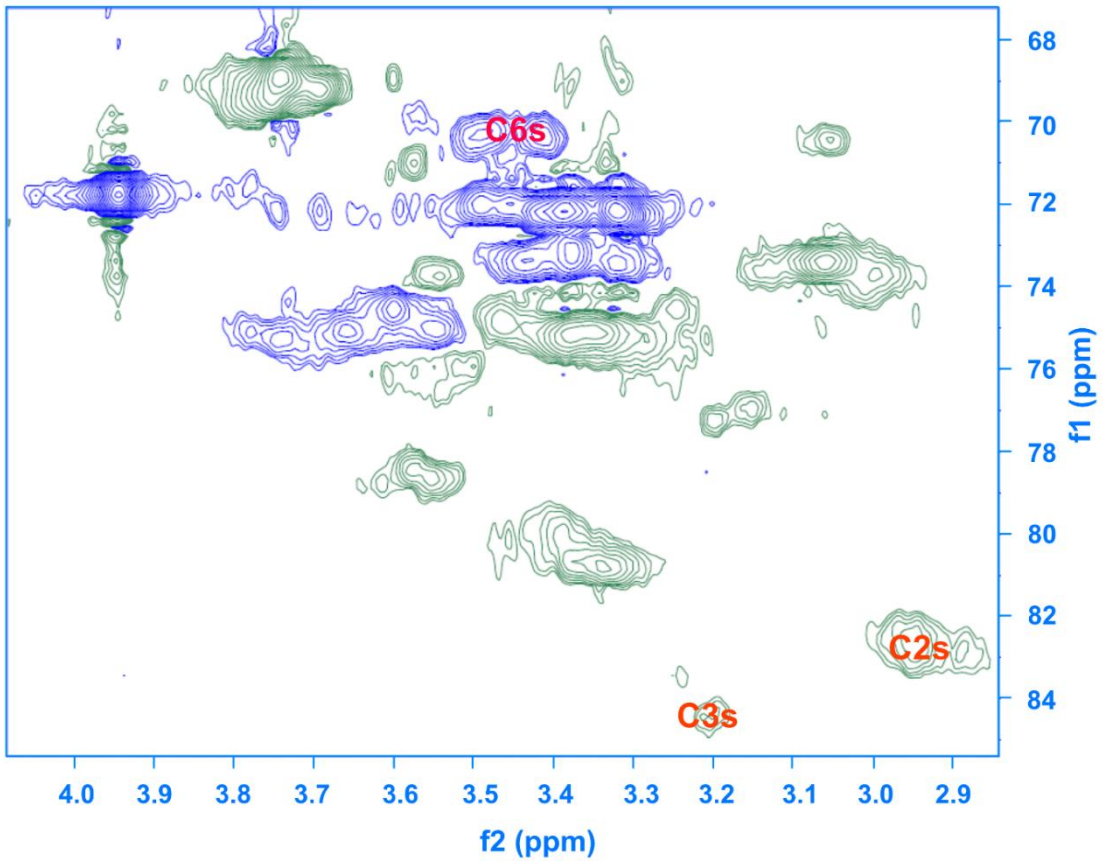


*Figure 22. HSQC NMR spectrum of AHP-cellulose synthesized in Triton B*

#### 6.1.4.1 Comparison of the substitution in different solvents

In order to estimate the substitution on AHP-cellulose the integral values of C11 and C1 as in quantitative $^{13}C$ NMR were used. This approach was taken since all C1 carbons,

including those shifted due to a nearby substitution, appeared between 100 and 105 ppm without any overlap of other peaks. It is important to note that in the selected model reaction of cellulose etherification via epoxy ring opening of AGE, a new OH group is introduced on position 8 of the substituent (figure 21a). This new OH group has the potential to react further with another AGE (through the so-called cascade reaction, figure 23). Thus, the summarized values in table 2 (calculated from $^{13}C$ NMR) were reported as molar substitution (MS), referring to the average number of moles of substituents introduced per each AGU ring. It is notable that the possibility exists for the same cascade reaction to occur in AGE hydrolysis side-reaction when a diol is formed, which leads to higher molecular structure that might be retained within cellulose during the dialysis work-up. Therefore, to make sure that the isolated AHP-cellulose did not contain any by-products from the side-reaction, AGE hydrolysis was performed in absence of MCC. Then the same work-up process was carried out to isolate any potential products. However, no by-products were obtained.

$$MS = \frac{C_{11}}{C_1}$$

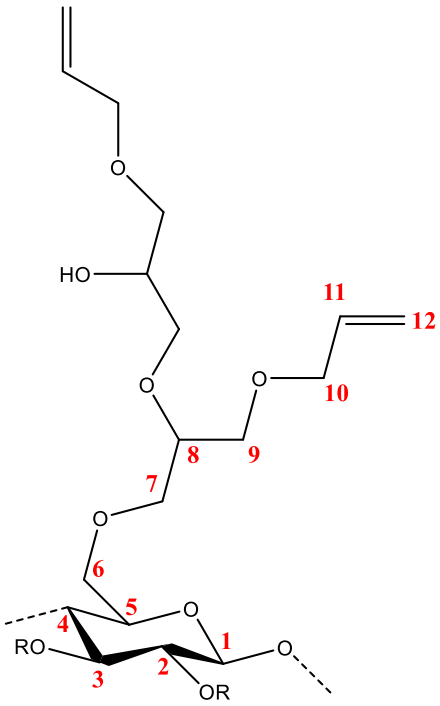


*Figure 23. Product of cascade reaction on C8*

*Table 2. Estimated MS calculated from $^{13}C$ NMR*

| Sample | MS |
|---|---|
| NaOH | 1.49 |
| TMAH | 0.88 |
| TMAH/Triton B | 0.81 |
| Triton B | 0.79 |
| Triton B/NaOH | 0.79 |
| TMAH/NaOH | 0.79 |

In addition, following the recent procedure reported by Kono et al.[90] efforts were made to evaluate the degree of substitution on individual cellulose carbons. However, in this study the estimation of the substitution distribution was not possible due to the heavy overlap of the signals and complex line shapes of the peaks.
The results in table 2 show that etherification in NaOH leads to the highest MS value of 1.49 while other solvents yielded lower and quite similar values of 0.79-0.88. Yet the question remains: Does this mean that cellulose is more substituted in NaOH compared to other solvents? To be able to answer this question previously obtained results need to be considered as well.

As mentioned before, evaluation of the HSQC spectra discloses that hydroxyl groups attached to C2, C3 and C6 have been functionalized with no significant deviations between the studied solvents. Moreover, AHP-cellulose obtained in NaOH had lower solubility in DMSO-$d_6$ compared to the other samples and its resulting $^{13}C$ NMR (figure 23 blue spectra) does not look significantly different compared to the other spectra (except for C1 and C6 with higher intensity). If the high value reported for NaOH(aq) had been an indication of more substitution on cellulose, a different spectrum would have been obtained with higher intensity of substituted C2, C3 and C6. Besides, according to the previous reports, upon increase in cellulose substitution, a decrease in the relative intensity of C1 and C6 is observed while the relative intensity of C1s and C6s increases[91,92]. However, $^{13}C$ NMR in NaOH shows higher intensity of C6 and C1 compared to the corresponding spectra in TMAH (figure 24, red). Therefore, considering the above mentioned results together with enhanced cellulose dissolution in TMAH and Triton B reported by Swensson et.al. [85,86], better solubility of AGE and higher temprature stability of solutions in all the solvents except in NaOH (where cellulose starts to precipitate when AGE reaches its maximum dissolution, figure 15 and table 1), might point out towards a more pronounced cascade reaction in NaOH(aq). When cellulose precipitates in NaOH, accessibility of cellulose hydroxyl groups to AGE decreases while in the other hand it is probable that the new hydroxide group formed on C8 (figure 21a) probably has more potential to react with another AGE, promoting the cascade reaction (resulting in high MS value). Yet, this hypothesis needs to be more investigated. It is noteworthy to state that the substitution pattern is likely uneven, since the yielded AHP-cellulose was not soluble in $D_2O$, which has also been reported before [93].

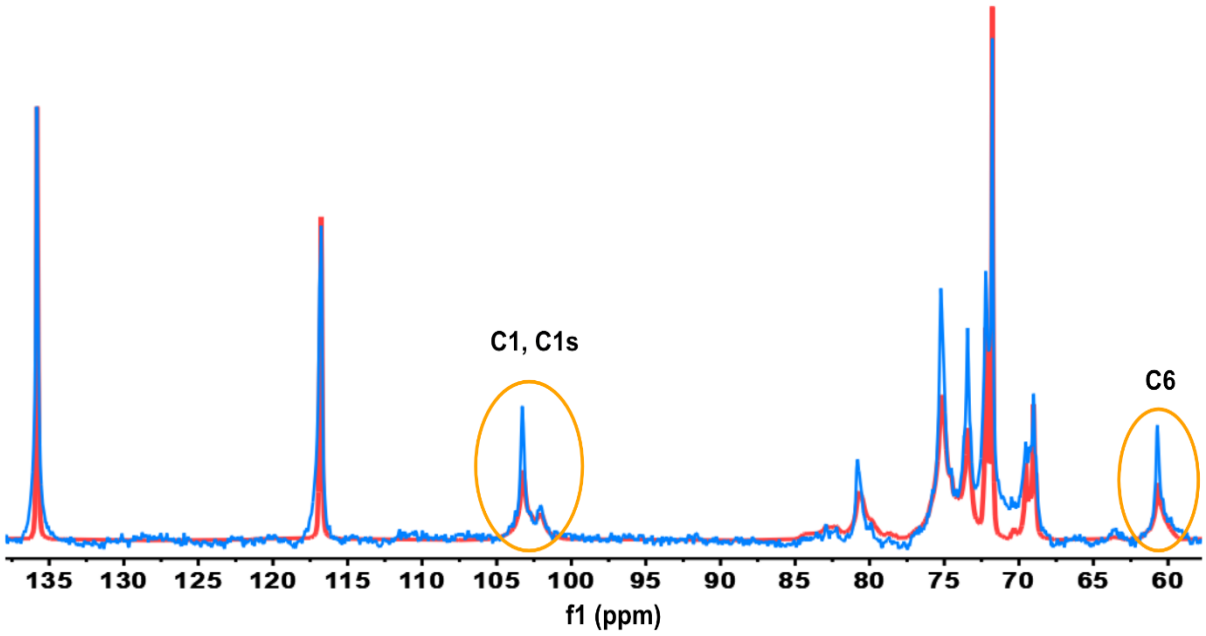


*Figure 24. $^{13}C$ NMR spectra of AHP-cellulose isolated from NaOH (blue) and TMAH (red)*

## 6.2 Aqueous *N,N*-dimethylmorpholinium hydroxide as a novel solvent for cellulose

In continuation to our previous study on cellulose etherification in two quaternary ammonium hydroxides (Triton B and TMAH) as well as NaOH, highlighting the importance of cellulose dissolution and since in the previous works of our group the favourable interactions of cellulose with quaternary ammonium hydroxides were presented, the second study aimed to develop a new quaternary ammonium hydroxide and investigate its potential towards cellulose dissolution. The inspiration was drawn from *N*-methylmorpholinium *N*-oxide, which is commercially used as a direct solvent for cellulose in Lyocell process, in addition to relatively low toxicity and good stability reported for ionic liquids based on morpholinium cations[44]. Therefore, by coupling *N,N*-dimethylmorpholinium with a hydroxide counterion, this study aimed at synthesizing *N,N*-dimethylmorpholinium hydroxide (NDMM-OH) in aqueous solution.

### 6.2.1 Development of a new hydroxide solvent for cellulose: NDMMO-OH, synthesis and characterisation

Development of a new hydroxide solvent for cellulose was inspired by the structure of the commercially used *N*-methylmorpholinium oxide (NMMO). For this purpose, a two-step procedure was taken for NDMM-OH synthesis: (1) methylation of *N*-methylmorpholine to yield *N,N*-dimethylmorpholinium iodide and, (2) an ion exchange step to replace iodide with hydroxide ion (Figure 25a). Figure 25b and 25c, as well as pH measured in the yielded aqueous NDMM-OH solution (14.7), confirmed the synthesis.

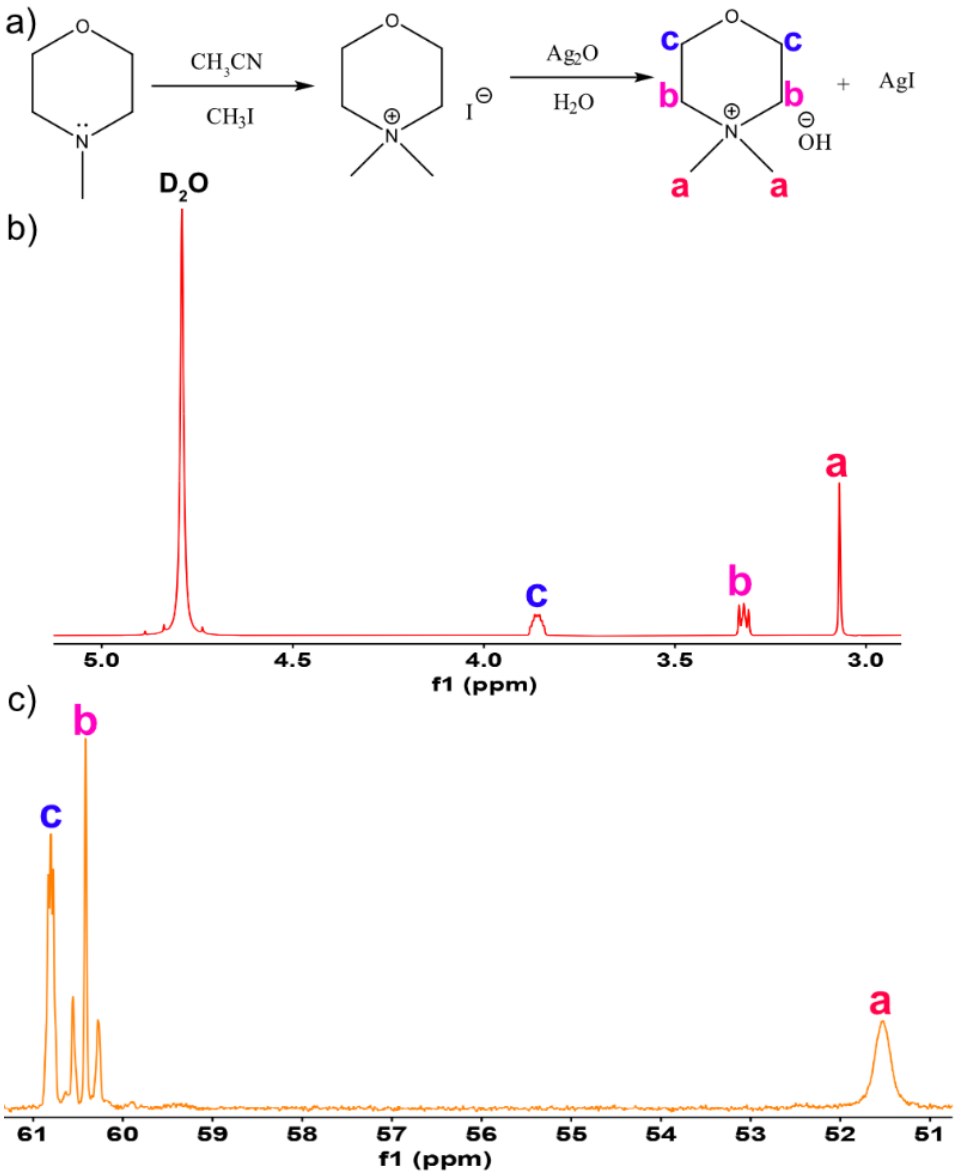


*Figure 25. a) Scheme of NDMM-OH synthesis and its corresponding b) $^{1}H$ NMR c) $^{13}C$ NMR spectra*

### 6.2.2 Cellulose dissolution in NDMM-OH(aq)

In the investigated concentration range of the solvent, from 0.8-2.3M, 1-2M NDMM-OH(aq) was indeed able to dissolve cellulose. As shown in figure 26, in this range, cellulose solutions were transparent and high transmittance of 92-96% in UV-Vis measurements as well as clear microscopy images were achieved. It is important to note that the presence of dust particles, microbubbles, traces of silver oxide or even a scratch on the measuring cell could have caused the transmittance to fall short of 100%. Yet, at lower concentration (0.8 M) and concentrations above 2 M, opaque solutions with low transmittance and microscopy images containing cellulose particles were yielded (figure 27).

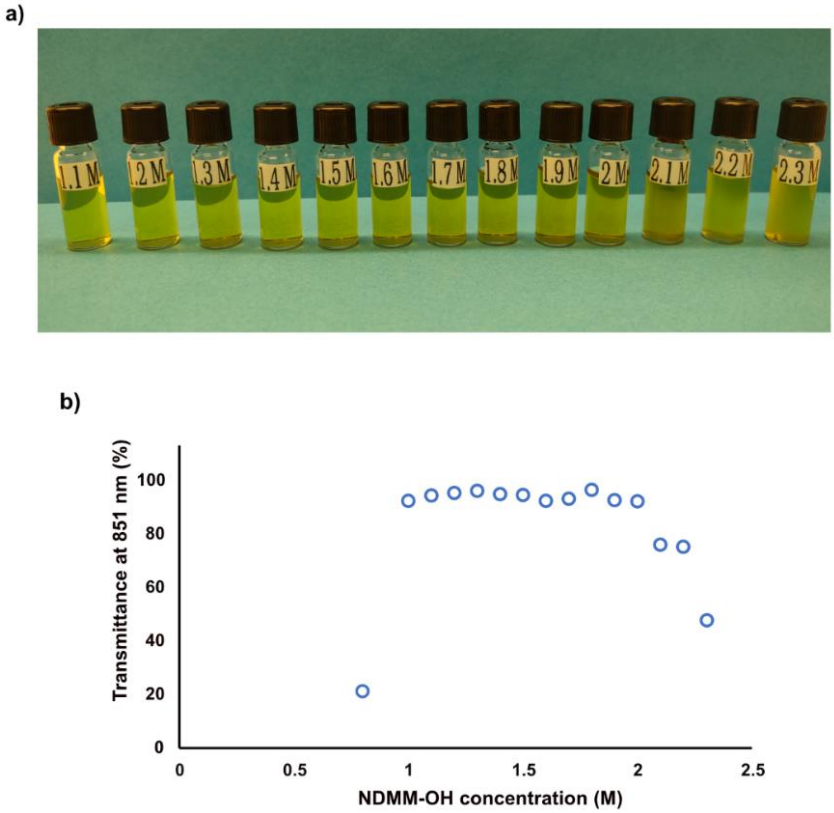


*Figure 26. a) MCC 3wt% in NDMM-OH(aq) 1.1-2.3 M from left to right b) Transmittance of the corresponding solutions at 851 nm*

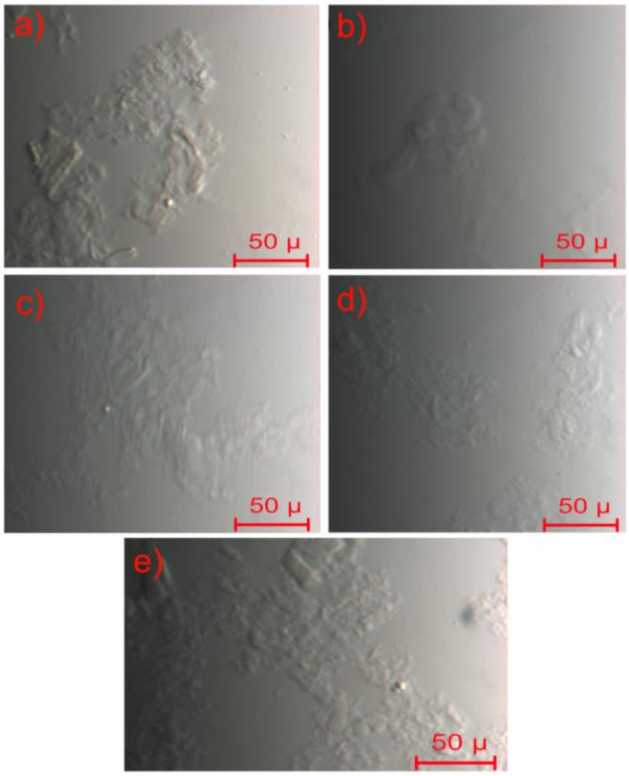


*Figure 27. Microscopy images of MCC 3 wt% in NDMM-OH(aq) a) 0.8 M, b) 2 M, c) 2.1 M, d) 2.2 M, e) 2.3 M*

The narrow concentration range allowing for cellulose dissolution has been commonly observed for aqueous solvents such as NaOH, which dissolves cellulose in the range of 1.5-2.5 M[56,94] . This is potentially due to specific required basicity for cellulose deprotonation (lower base concentration limit), and certain hydration of ions (higher concentration limit). It is probable that solvated ions of a particular hydrodynamic diameter are required to accomplish dissolution by stabilizing the dissolved chains.

Initial investigations on MCC dissolution at higher temperatures (5 °C, room temperature and 38°C) did not result in dissolution but rather cellulose suspensions (figure 28).

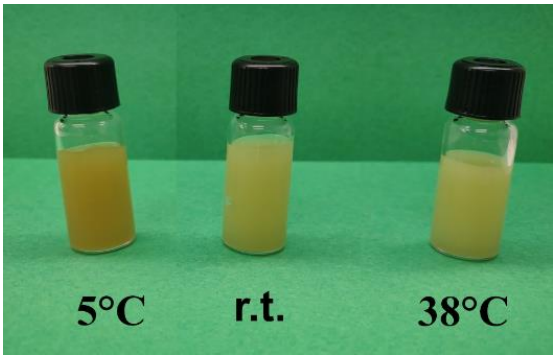


*Figure 28. MCC 3wt% in 1.3 NDMM-OH at, 5 °C, room temperature and 38 °C*

#### 6.2.2.1 Maximum MCC dissolution in NDMM-OH(aq)

To assess dissolution capacity of NDMM-OH(aq), cellulose solutions with increasing MCC concentrations were prepared in 1.3 M NDMM-OH(aq). As depicted in figure 29, up to 7 wt% MCC could be dissolved resulting in clear microscopy images and high transmittance while at concentrations above 7 wt% cellulose solutions immediately gelled and cellulose particles could be easily detected by microscopy. These values are comparable to the maximum dissolution capacity of NaOH(aq). In one study, maximum 5 wt% MCC was initially dissolved in NaOH(aq) 2.3 M and then diluted to 1.3 M[95] while in another study, maximum 2 wt% MCC could be dissolved in 2 M NaOH [96].

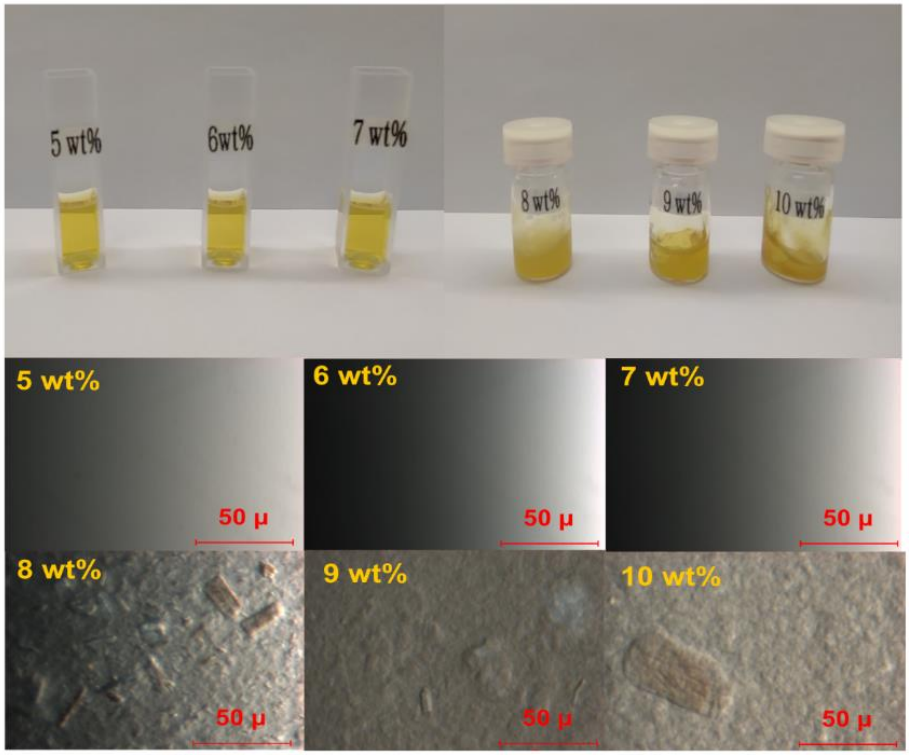


*Figure 29. Varying amounts of MCC in NDMM-OH(aq) 1.3 M and their corresponding microscopy images*

### 6.2.3 Pulp dissolution in NDMM-OH(aq)

The new solvent proved to also be capable of dissolving pulp. When pulp fibres are added to aqueous hydroxides, they initially go through a ballooning step, which includes heterogeneous swelling and partial dissolution of the differently oriented cellulose microfibrils layers in the fibre walls. This could be observed when adding NDMM-OH(aq) to two different types of dissolving pulp: a hardwood pulp, visc. 283 $cm^3/g$ (pulp A) and a softwood pulp, visc. 442 $cm^3/g$ (pulp B). As depicted in figure 30, the dissolution of 0.5 wt% pulp A resulted in 92.4% transmittance and traces of ballooning structures in microscopy images and 1 wt% pulp A led to 77% transmittance and a few more ballooning in the fibres. It was also observed that increasing NDMM-OH(aq) concentration to 1.6 M or an additional freeze-thaw step when dissolving 1 wt% pulp A, enhanced the transmittance to 84.6% and 86.5%, respectively. Furthermore, dissolution of 0.5 wt% and 1 wt% pulp B in 1.3 M NDMM-OH(aq) yielded solutions showing 83.8% and 76.6% transmittance, respectively, as well as few fibre ballooning.

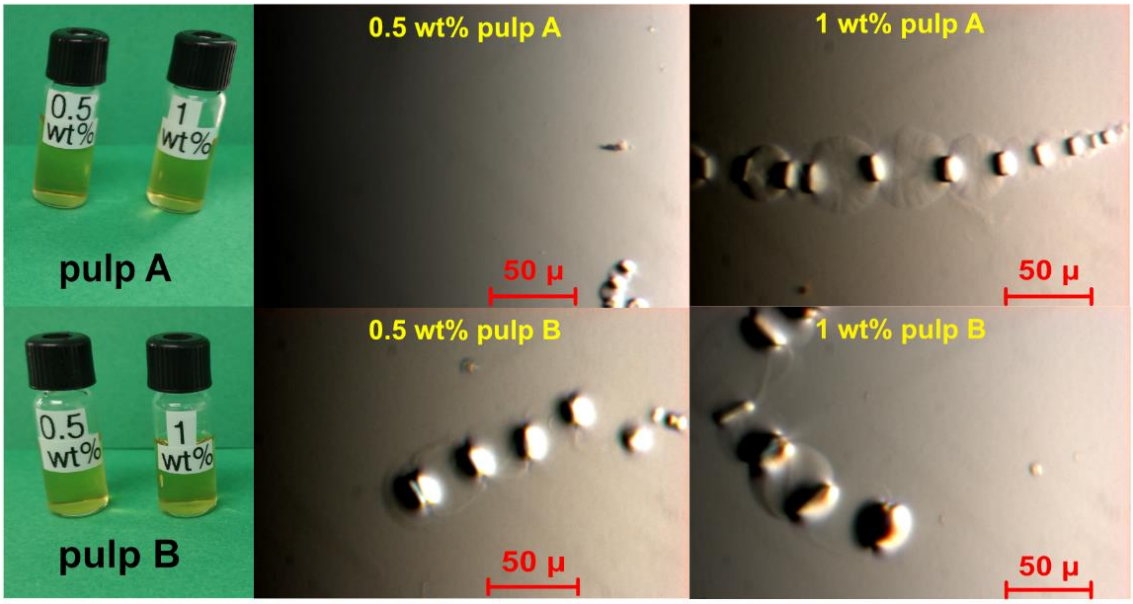


*Figure 30. Dissolution of pulp in 1.3 M NDMM-OH*

### 6.2.4 Chemical stability of cellulose dissolved in NDMM-OH(aq)

As shown in figure 31a, when cellulose was dissolved in NDMM-OH(aq) the solution turned yellow. The appearance of a yellow color in alkaline solutions is typically a sign of degradation. Hence, to assess the chemical stability of cellulose in this solvent, molecular weight distribution of dissolved cellulose, as well as molecular structure of the solution components after storage, were analysed by SEC in DMAc/LiCl and $^{13}C$ NMR.

For molecular weight analysis cellulose precipitated from a 3 wt% solution in 1.3 M NDMM-OH(aq) was SEC-analysed and compared to both an MCC reference and MCC precipitated from 2.1 M NaOH(aq) (refrigerated for 15 h). As figure 31 shows, the shape of the obtained chromatograms looks nearly identical. Furthermore, the polydispersity (PD) values do not differ significantly (figure 31, table b). However, the values in the table show a slight decrease in Mw, interpreted as minor cellulose degradation likely due to the reducing end chemistry and beta elimination, which is commonly observed in alkaline systems with good cellulose accessibility.

a)

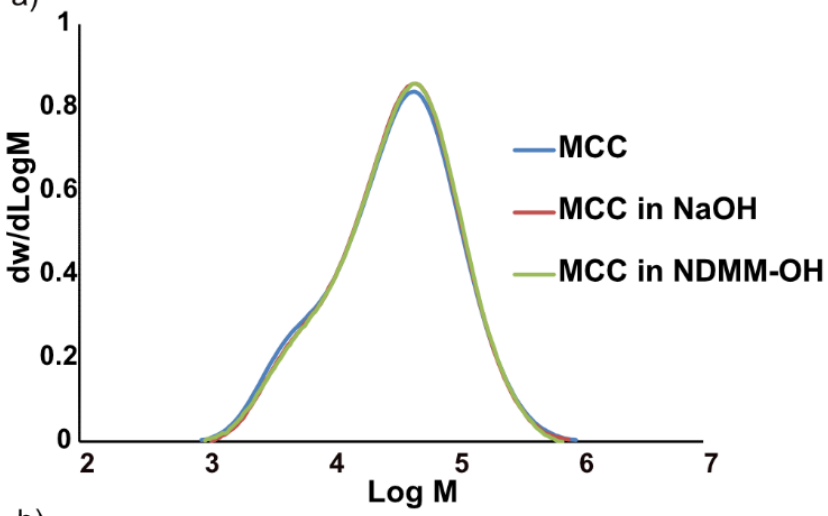


b)

| Sample name | Mw (kg/mol) | Mp (kg/mol) | Mn (kg/mol) | Mv (kg/mol) | PD |
|---|---|---|---|---|---|
| MCC | 60.6 | 48.1 | 16.0 | 139.0 | 3.8 |
| MCC in NaOH | 60.3 | 49.2 | 17.3 | 131.6 | 3.5 |
| MCC in NDMM-OH | 59.7 | 47.0 | 17.0 | 125.0 | 3.5 |

*Figure 31. a) Molecular weight distribution (determined by SEC in DMAc/LiCl) for MCC reference (blue) and MCC samples dissolved and precipitated after 15h storage from NDMM-OH (green) and NaOH (orange) b) Detailed analysis values*

$^{13}$C NMR measurements were run on freshly dissolved MCC in NDMM-OH(aq) as well as an aged sample that had been refrigerated for 16 h after dissolution (figure 32). Both spectra look identical: there are 8 distinct peaks at 103.78, 79.22, 75.53, 75.21 and 73.86 ppm assigned to C1, C4, C5, C3 and C2 positions in cellulose, respectively. In addition, the three other peaks at 60.90, 60.51 and 51.64 ppm correspond to NDMM-OH. No extra peaks or shifts could be detected upon storage, indicating absence of any detectable degradation. It should be noted that C6 in cellulose appears at around ca. 60 ppm, which overlaps with NDMM-OH peaks.

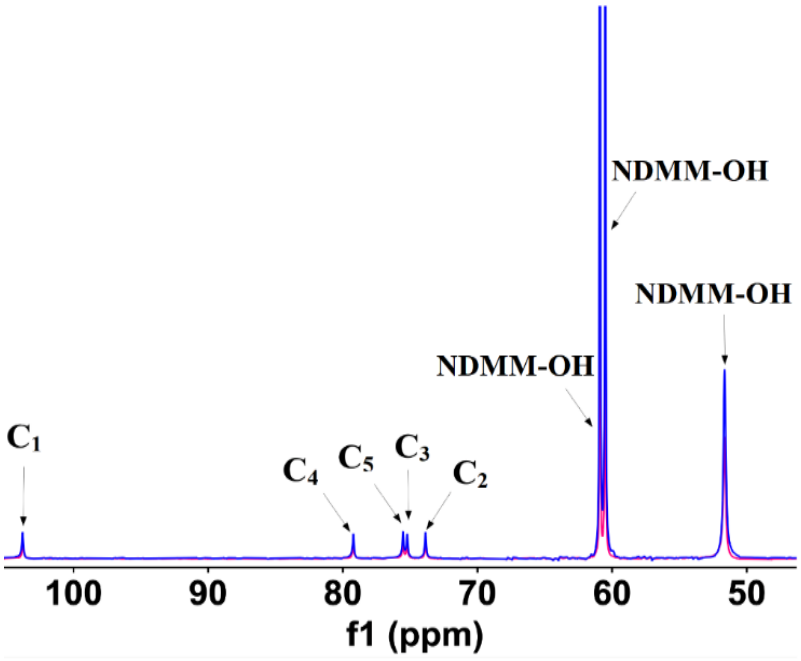


*Figure 32. $^{13}C$ NMR measurements of freshly dissolved MCC 3 wt% in NDMM-OH(aq) (pink) and an aged solution refrigerated for 16h post dissolution (blue)*

### 6.2.5 Assessment of cellulose solution properties in NDMM-OH(aq)

#### 6.2.5.1 Intrinsic viscosity

A good quality solvent leads to the extension of the dissolving polymer. The quality of the solvent can be investigated by intrinsic viscosity measurements, where a higher intrinsic viscosity ($\eta_{sp}/C$) is an indication of a more extended polymer, and therefore a better solvent. Figure 33 shows $\eta_{sp}/C$ vs C used to extrapolate the intrinsic viscosity value of 1.11 dL/g. In previous work of our group[85] intrinsic viscosity values of 1.14, 0.88 and 0.92 dL/g were reported when cellulose was dissolved in 2.3 M TMAH(aq), NaOH(aq) as well as TMAH/NaOH, respectively. The obtained value for NDMM-OH(aq) is comparative to the values reported for TMAH and TMAH/NaOH, and slightly higher than the value reported for NaOH. This indicates a similar stabilizing interaction between cellulose and these solvents.

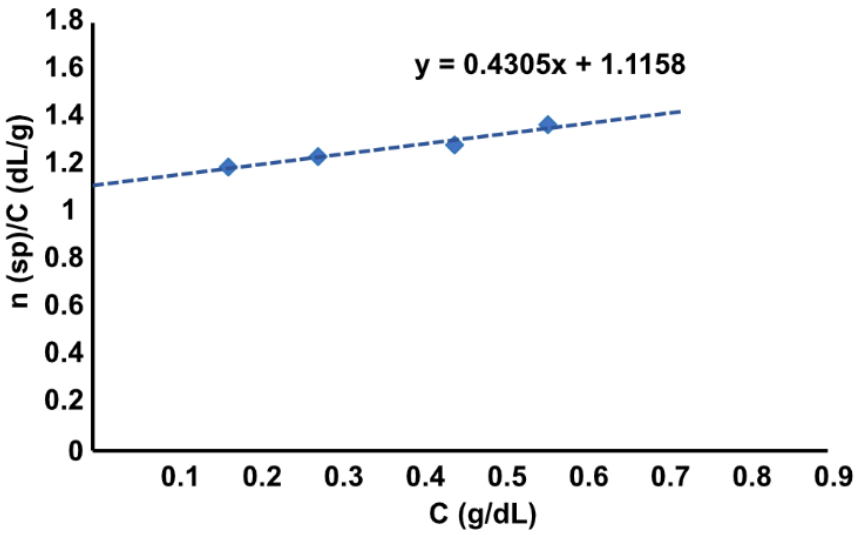


*Figure 33. Intrinsic viscosity extrapolated from $\eta_{sp}/C$ plotted vs. C g/dL in 1.3 M NDMM-OH*

#### 6.2.5.2 Dynamic light scattering (DLS)

To evaluate whether cellulose is molecularly dissolved in NDMM-OH(aq), DLS measurements were run to obtain the hydrodynamic radius of cellulose at dilute concentrations. To separate different populations of cellulose, a distribution fit was applied (figure 34). Figure 34a and 34b are representative of an unfiltered and filtered (with a 0.22 µm filter) MCC 0.5 wt% sample, respectively. The results in figure 34a and table c show three populations, one of which consists of larger particles likely to be indicative of aggregates. It is necessary to note that dust particles could cause contamination in unfiltered sample. However, the majority of the population in the unfiltered sample includes smaller particles of approximately 10 nm in size, that is in a good correlation with the expected size of molecularly dissolved MCC chains[97]. Analysis of figure 34b and table d results in two populations for the filtered sample: the molecularly dissolved cellulose similar to the unfiltered sample, and an even smaller fraction. Since cellulose is polydisperse the latter fraction potentially originated from the shorter chains (also indicated by the polydispersity index).

a)

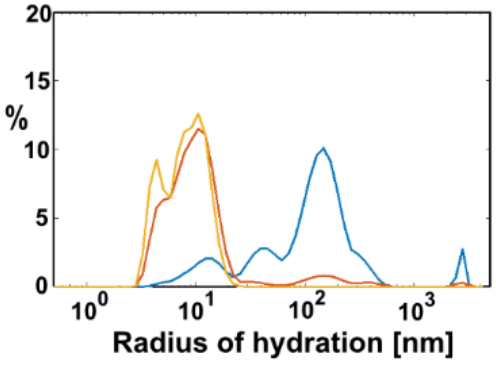


b)

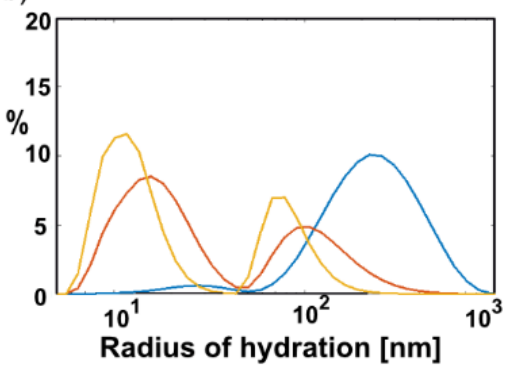


c)


| Unfiltered solution | Peak 1*R (%) [nm] | Peak 2 R (%) [nm] | Peak 3 R (%) [nm] |
|---|---|---|---|
| Intensity | 164±79 (68.7%) | 42±11 (15.1%) | 13±4 (12.9%) |
| Volume | 10±6 (92.8%) | 159±60 (5.4%) | 400±78 (1.1%) |
| Number | 10±3 (69.5%) | 4.6±0.8 (30.5%) | - |

* Radius

d)

| Filtered, 0.22 µm | Peak 1 R (%) [nm] | Peak 2 R (%) [nm] |
|---|---|---|
| Intensity | 26±14 (96%) | 3±1 (4%) |
| Volume | 13±7 (36%) | 2±1 (64%) |
| Number | 9±3 (33.4%) | 1±0.5 (66.6%) |

*Figure 34. a) Unfiltered sample of 0.5 wt% MCC in 1.3 M NDMM-OH(aq) and b) Filtered sample of 0.5 wt% MCC in 1.3 M NDMM-OH(aq). Tables: distribution analysis of c) unfiltered sample of 0.5 wt.% MCC in 1.3 M NDMM-OH(aq) and d) filtered sample of 0.5 wt.% MCC in 1.3 M NDMM-OH(aq)*

# 7 Conclusions

*In-situ* monitoring of cellulose etherification in aqueous alkaline solutions is challenging due to the extensively occurring side reactions (hydrolysis and cascade reactions of the etherifying agent), instability of the cellulose solutions and multiple overlapping signals. Nevertheless, *in-situ* IR spectroscopy can provide us with valuable insights on hydrolysis of the reagent, estimating the endpoints of the reactions and stability of solutions during the reaction complemented with *in-situ* viscosity measurements. In this study the role of solvent for cellulose reactivity towards modification has been highlighted indicating higher temperature stability of cellulose solutions in Triton B(aq) and TMAH(aq), enhanced dissolution of the etherifying reagent of interest (AGE) and speeding up the overall reaction compared to NaOH(aq). NMR analysis together with the observations and obtained results indicated extensive cascade reaction in NaOH(aq) due to low AGE solubility, low temperature stability of cellulose solution and thus lower accessibility of cellulose OH groups compared to those freshly formed on the introduced substituents. These results together stress the critical role of solvent and the impact of the hydroxide base composition on cellulose modification.

Furthermore, *N,N*-dimethylmorpholinium hydroxide (NDMM-OH(aq)) was synthesized and proved to be capable of dissolving both microcrystalline cellulose (MCC) and pulp (with traces of fibres ballooning detected in pulp). Cellulose solutions in NDMM-OH(aq) were chemically stable after refrigeration for 15-16h and contained predominantly molecularly dissolved cellulose. Finally, similar nature of stabilizing solvent-cellulose interactions to other aqueous hydroxide solvents was indicated by intrinsic viscosity measurements.

# 8 Future work

In the future work, efforts will be made to further understand properties of QAHs(aq) as functionalisation media for cellulose. The molecular interactions between cellulose and NDMM-OH(aq), TMAH and Triton B will be investigated, which will give a deeper insight into the mechanism of cellulose dissolution in QAHs(aq). In addition, cellulose dissolution in NDMM-OH(aq) under varying dissolution conditions will be assessed thoroughly, as there have been several reports on the potential of QAHs in cellulose dissolution at broader concentration and temperature ranges compared to NaOH(aq). Since the new solvent—NDMM-OH(aq)—opens up new opportunities for cellulose modification (whether through regeneration or functionalization), chemical functionalisation routes in this solvent will be investigated.

# 9 Acknowledgements

-Knut and Alice Wallenberg Foundation within Wallenberg Wood Science Center is acknowledged gratefully for funding this project.

In addition, I wish to express my deepest gratitude to:

-My main supervisor Merima Hasani and my co-supervisor Diana Bernin not only for fruitful discussions, supporting and encouraging me but also for having faith in my abilities and making this work possible.

-My examiner Hans Theliander and all of my colleagues at SIKT for their support and help. Thanks for making the work much more fun.

-Paul Kuijpers for great discussions and help with *in-situ* IR study.

-Sylwia Wojno and Roland Kádár for running rheology measurements and very helpful discussions.

-Ulrika Brath for valuable discussions on NMR results and Swedish NMR centre for providing spectrometer time

-Malin Larsson for your kind and friendly support, you are amazing with a golden heart Malin!

-My friends at Chalmers with whom I spent very nice times.

-Last but not least my family, for encouraging me to move to Sweden, for keeping your faith in me and supporting me though from a long distance, and Soheil who always backed me up in hardships, stayed positive and kept telling me “I am proud of you Shirin” which indeed refilled my energy.

# 10 References


1 A. Payen and C. R. Hebd, *Seances Acad. Sci.*, 1838, **7**, 1125.
2 A. Payen and C. R. Hebd, *Seances Acad. Sci.*, 1838, **7**, 1052.
3 A. Brogniart, A. Pelonze and R. Dumas, *Comptes Rendus*, 1839, **8**, 51 – 53.
4 H. Staudinger, *Ber. Dtsch. Chem. Ges.*, 1920, **53**, 1073–1085.
5 B. Medronho and B. Lindman, *Adv. Colloid Interface Sci.*, 2015, **222**, 502–508.
6 B. Hinterstoisser and L. Salmén, *Vib. Spectrosc.*, 2000, **22**, 111–118.
7 J. W. S. Hearl, *J. Polym. Sci.*, 1958, **XXVIII**, 432–435.
8 V. L. Finkenstadt and R. P. Millane, *Macromolecules*, 1998, **31**, 7776–7783.
9 P. Langan, Y. Nishiyama and H. Chanzy, *Biomacromolecules*, 2001, **2**, 410–416.
10 E. S. Gardiner and A. Sarko, *Can. J. Chem.*, 1985, **63**, 173–180.
11 H. J, S. A, O. J and W. S, *Polym Sci Polym Lett*, 1975, **13**, 23–27.
12 A. Chami Khazraji and S. Robert, *J. Nanomater.*, 2013, **2013**, 1–10.
13 K. Jedvert and T. Heinze, *J. Polym. Eng.*, 2017, **37**, 845–860.
14 D. Fengel and G. Wegener, *Wood: Chemistry, Ultrastructure, Reactions.*, De Gruyter, Inc., Berlin/Boston, Germany, 1983.
15 A. M. Boudet, *Plant Physiol. Biochem.*, 2000, **38**, 81–96.
16 H. Sixta, in *Handbook of pulp*, Wiley-VCH Verlag GmbH & Co., 2006, p. 1010.
17 D. Li, D. Ibarra, V. Köpcke and M. Ek, in *In Functional Materials from Renewable Sources*, American Chemical Society, 2012, pp. 167–189.
18 D. Klemm, B. Heublein, H. P. Fink and A. Bohn, *Angew. Chemie - Int. Ed.*, 2005, **44**, 3358–3393.
19 V. Köpcke, KTH Royal Institute of Technology, 2008.
20 H. A. Krässig, *Cellulose, Structure, Accessibility and Reactivity*, Gordon and Breach Publishers, Amsterdam, 1993.
21 F. R. Amin, H. Khalid, H. Zhang, S. Rahman, R. Zhang, G. Liu and C. Chen, *AMB Express*, 2017, **7**, 1–12.
22 B. Volkert, W. Wagenknecht and M. Mai, *ACS Symp. Ser.*, 2010, **1033**, 319–341.
23 T. Liebert, D. Klemm and T. Heinze, *J. Macromol. Sci. Part A Pure Appl. Chem.*, 1996, **33**, 613–626.
24 D. Klemm, T. Heinze, B. Philipp and W. Wagenknecht, *Acta Polym.*, 1997, **48**, 277–297.
25 T. Heinze, O. A. El Seoud and A. Koschella, in *Cellulose Derivatives*, publisher, 2018, pp. 293–427.
26 Fabric series: All about Viscose, https://kleiderly.com/blogs/kleiderly-magazine/fabric-series-all-about-viscose.

27 G. J. Askew, H. S. Bahia, C. W. Foxall, S. J. Law, H. Street, WO 98/28360, 1998, 1–24.
28 D. L. Johnson, US3508941A, 1970.
29 H. Chanzy, S. Nawrot, A. Peguy and P. Smith, *J. Polym. Sci.*, 1982, **20**, 1909–1924.
30 T. Rosenau, A. Potthast, H. Hettegger, M. Bacher, M. Opietnik, T. Röder and I. Adorjan, *Cellulose*, 2021, **28**, 10143–10161.
31 M. Michael, R. N. Ibbett and O. W. Howarth, *Cellulose*, 2000, **7**, 21–33.
32 E. R. Maia and S. Perez, *Nov J Chim*, 1983, **7**, 89–100.
33 T. Rosenau, A. Potthast, H. Sixta and P. Kosma, *Prog. Polym. Sci.*, 2001, **26**, 1763–1837.
34 F. Wendler, A. Kolbe, F. Meister and T. Heinze, *Macromol. Mater. Eng.*, 2005, **290**, 826–832.
35 F. Wendler, G. Graneß and T. Heinze, *Cellulose*, 2005, **12**, 411–422.
36 F. Wendler, G. Graneß, R. Büttner, F. Meister and T. Heinze, *J Polym Sci, Part B Polym Phys*, 2006, **44**, 1702–1713.
37 A. J. Sayyed, N. A. Deshmukh and D. V. Pinjari, *Cellulose*, 2019, **26**, 2913–2940.
38 C. Graenacher, US1943176A, 1934.
39 J. Zhang, Q. Ren and J. S. He, CN Pat., ZL02155945, 2002.
40 A. Xu, J. Wang and H. Wang, *Green Chem.*, 2010, **12**, 268–27.
41 Y. Fukaya, A. Sugimoto and H. Ohno, *Biomacromolecules*, 2006, **7**, 3295–3297.
42 A. Brandt, M. J. Ray, T. Q. To, D. J. Leak, R. J. Murphy and T. Welton, *Green Chem.*, 2011, **13**, 2489–2499.
43 B. Zhao, L. Greiner and W. Leitner, *RSC Adv.*, 2012, **2**, 2476–2479.
44 D. G. Raut, O. Sundman, W. Su, P. Virtanen, Y. Sugano, K. Kordas and J. P. Mikkola, *Carbohydr. Polym.*, 2015, **130**, 18–25.
45 R. S. Payal, R. Bharath, G. Periyasamy and S. Balasubramanian, *J. Phys. Chem. B*, 2012, **116**, 833–840.
46 G. Bentivoglio, R. Thomas, M. Fasching, M. Buchberger, H. Schottenberger and H. Sixta, *Lenzinger Berichte*, 2006, **86**, 154–161.
47 B. Kosan, C. Michels and F. Meister, *Cellulose*, 2008, 59–66.
48 L. Feng and Z. Chen, *J. Mol. Liq.*, 2008, **142**, 1–5.
49 E. S. Sashina, *Fibre Chem.*, 2007, **39**, 153–158.
50 W. Traube, *Ber Dtsch Chem Ges*, 1912, **44**, 3319–3324.
51 A. D. Bain, *Carbohydr Res*, 1980, **84**, 1–12.
52 J. Burger, G. Kettenbach and P. Klüfers, *Macromol Symp*, 1995, **95**, 113–126.
53 R. Ahlrichs, M. Ballauff, K. Eichkorn, O. Hanemann, G. Kettenbach and P. Klufers, *Chem Eur J*, 1998, **4**, 835–844.
54 F. Wurm, B. Rietzler, T. Pham and T. Bechtold, *Molecules*, 2020, **25**, 1840.
55 L. Lilienfeld, US1771462A, 1930.
56 H. Sobue, H. Kiessig and K. Hess, *Z Phys Chem B*, 1939, 309–328.
57 T. Budtova and P. Navard, *Cellulose*, 2016, **23**, 5–55.
58 S. Väisänen, R. Ajdary, M. Altgen, K. Nieminen, K. K. Kesari, J. Ruokolainen, O. J. Rojas and T. Vuorinen, *Cellulose*, 2021, **28**, 1267–1281.
59 B. Xiong, P. Zhao, K. Hu, L. Zhang and G. Cheng, *Cellulose*, 2014, **21**, 1183–1192.
60 H. Jin, C. Zha and L. Gu, *Carbohydr. Res.*, 2007, **342**, 851–858.
61 L. Yan and Z. Gao, *Cellulose*, 2008, **15**, 789–796.
62 D. H. Powers, L. H. Bock, US2009015A, 1935, 1–4.

63 R. Ehert and V. T. Lieser, *Viscositiitsuntersuchungen an Cellul.*, 1937, **532**, 94–103.
64 T. Brownsett and D. A. Clibbens, *J. Text. Inst. Trans.*, 1941, **32**, T57–T70.
65 T. Brownsett and D. A. Clibbens, *J. Text. Inst. Trans.*, 1941, **32**, T32–T44.
66 S. M. Hudson and J. A. Cuculo, *J. Macromol. Sci.*, 1980, **18**, 1–82.
67 C. Zhong, C. Wang, F. Huang, H. Jia and P. Wei, *Carbohydr. Polym.*, 2013, **94**, 38–45.
68 M. Abe, T. Yamada and H. Ohno, 2014, **4**, 17136–17140.
69 U. Hyväkkö and I. King, Alistair W. T. Kilpeläinen, *bioresources*, 2014, **9**, 1565–1577.
70 M. Gubitosi, H. Duarte, L. Gentile, U. Olsson and B. Medronho, *Biomacromolecules,* 2016, **17**, 2873–2881.
71 M. Abe, Y. Fukaya and H. Ohno, *chem.commun.*, 2012, 48, 1808–1810.
72 A. Tsurumaki, M. Tajima, M. Abe, D. Sato and H. Ohno, *Phys. Chem. Chem. Phys.*, 2020, **22**, 22602–22608.
73 Y. Wang, L. Liu, P. Chen, L. Zhang and A. Lu, *Phys. Chem. Chem. Phys.*, 2018, **20**, 14223–14233.
74 B. Lindman, G. Karlström and L. Stigsson, *J. Mol. Liq.*, 2010, **156**, 76–81.
75 O. A. El Seoud, H. Nawaz and E. P. G. Arêas, 2013, **18**, 1270–1313.
76 H. Nawaz, R. Casarano and O. A. El Seoud, *Cellulose*, 2012, **19**, 199–207.
77 A. Chadlia and M. H. M. Farouk, *J. Appl. Polym. Sci.*, 2011, **119**, 3372–3381 (2011).
78 J. Zhou, L. Zhang, Q. Deng and X. Wu, *J. Polym. Sci. Part A Polym. Chem.*, 2004, **42**, 5911–5920.
79 J. Zhou, Y. Qin, S. Liu and L. Zhang, *Macromol. Biosci.*, 2006, **6**, 84–89.
80 Y. Song, J. Zhou, L. Zhang and X. Wu, *Carbohydr. Polym.*, 2008, **73**, 18–25.
81 J. Zhou, C. Chang, R. Zhang and L. Zhang, *Macromol. Biosci.*, 2007, **7**, 804–809.
82 C. Chang, L. Zhang, J. Zhou, L. Zhang and J. F. Kennedy, *Carbohydr. Polym.*, 2010, **82**, 122–127.
83 X. Qin, A. Lu and L. Zhang, *Cellulose*, 2013, **20**, 1669–1677.
84 J. A. Sirvio and J. P. Heiskanen, *Cellulose*, 2020, **27**, 1933–1950.
85 B. Swensson, A. Larsson and M. Hasani, *Cellulose*, 2020, **27**, 101–112.
86 B. Swensson, A. Larsson and M. Hasani, *Polymers*, 2020, **12**, 1310.
87 B. J. Ha and S. Park, *Biomater. Res.*, 2018, **22**, 202–209.
88 H. Qi, T. Liebert and T. Heinze, 2012, 925–932.
89 J. Duanmua, E. K. Gamstedt and A. Rosling, *Starch*, 2007, **59**, 523–532.
90 H. Kono and J. Numata, *Carbohydr. Res.*, 2020, **495**, 108067.
91 T. Miyamoto, Y. Sato, T. Shibata and H. Inagaki, *J. Polym. Sci.*, 1984, **22**, 2363–2370.
92 S. Takahashi, T. Fujimoto and B. M. Barua, *J. Polym. Sci. Part A Polym. Chem.*, 1986, **24**, 2981–2993.
93 S. Richardson and L. Gorton, 2003, **497**, 27–65.
94 K. Kamide, K. Yasuda, T. Matsui, K. Okajima and T. Yamashiki, *Cellul Chem Technol*, 1990, **24**, 23–31.
95 A. Isogai and R. H. Atalla, *Cellulose*, 1998, **5**, 309–319.
96 B. Martin-Bertelsen, E. Andersson, L. Stigsson and U. Olsson, *Polymers*, 2020, **12**, 1–15.
97 K. Saalwächter, W. Burchard, P. Klüfers, G. Kettenbach, P. Mayer, D. Klemm and S. Dugarmaa, *Macromolecules*, 2000, **33**, 4094–4107.